REMOTE SENSING FOR MANAGEMENT OF INVASIVE PLANTS IN GREAT LAKES COASTAL WETLANDS

by

Matthew James Unitis

A thesis

submitted in partial fulfillment

of the requirements for the degree of

Master of Science in Biology

Boise State University

August 2018

BOISE STATE UNIVERSITY GRADUATE COLLEGE

DEFENSE COMMITTEE AND FINAL READING APPROVALS

of the thesis submitted by

Matthew James Unitis

Thesis Title: Remote Sensing for Management of Invasive Plants in Great Lakes Coastal Wetlands

Date of Final Oral Examination: 13 June 2018

The following individuals read and discussed the thesis submitted by student Matthew James Unitis, and they evaluated his presentation and response to questions during the final oral examination. They found that the student passed the final oral examination.

Jodi Brandt, Ph.D.	Chair, Supervisory Committee
Ian C. Robertson, Ph.D.	Member, Supervisory Committee
Stephen Novak, Ph.D.	Member, Supervisory Committee

The final reading approval of the thesis was granted by Jodi Brandt, Ph.D., Chair of the Supervisory Committee. The thesis was approved by the Graduate College.

DEDICATION

This thesis is dedicated to my parents, who have provided unconditional support throughout my life. Also to the support of the rest of my family, including my late Grandmother Florence who rolled her eyes at “muck work” but still took me to ponds and parks in my childhood.

ACKNOWLEDGEMENTS

This research was supported by the Michigan Department of Natural Resources through the Michigan Invasive Species Grant program. I would like to acknowledge the contributions and field work conducted by Shane Lishawa and Drew Monks of the Tuchmann lab at Loyola University Chicago. Dennis Albert and the Great Lakes Coastal Wetland Monitoring Program provided crucial knowledge and spatial data for the completion of the field studies. Laura Chavez and Michael Battaglia from the Michigan Tech Research Institute were instrumental in providing guidance in SAR processing and application.

ABSTRACT

Great Lakes coastal wetlands are some of the most crucial ecosystems to biodiversity in the Great Lakes Basin, yet suffer increasing degradation due to invasive plants. Wetland plant invasions can be controlled in their initial stages, but early detection of invasive plants using field surveys are often untenable due to budget constraints. Remote sensing techniques offer solutions to management objectives during the early stages of invasion on a landscape scale due to their ability to cheaply create spatially explicit information about plant distributions. Some invasive plants, such as *Typha x. glauca,* are conspicuous on a large scale, and can be mapped to their current extent using new satellite and modeling techniques. Inconspicuous invasive plants however, such as *Hydrocharis morsus-ranae,* may be undetectable by remote sensing sources and require predictive strategies. In this thesis I explored the use of remote sensing in the management of a conspicuous and inconspicuous invasive wetland plants in the St. Mary's River, MI. I successfully classified the current extent of conspicuous *Typha x. glauca* and other wetland vegetation types to provide spatially explicit maps for early detection and management and examined methods that can be adapted for use in emergent wetlands worldwide. The habitat suitability of inconspicuous *Hydrocharis morsus-ranae* was also determined using novel fine-scale habitat covariates determined from lidar and radar. Habitat covariates derived from these sources should see wider use in species distribution modeling, particularly with wetland plants, to create better predictions of invasive plant expansions. Implementation of new and upcoming remote

sensing data sources and methods will allow for better invasive wetland plant management at greater spatial and temporal scales than field studies alone.

TABLE OF CONTENTS

LIST OF TABLES

LIST OF FIGURES

LIST OF ABBREVIATIONS

BSU	Boise State University
GC	Graduate College
TDC	Thesis and Dissertation Coordinator
SAR	Synthetic Aperture Radar
SDM	Species Distribution Model
MDA	Mean Decrease in Accuracy
NIR	Near Infrared
MLE	Maximum Likelihood Estimation
UAV	Unmanned Aerial Vehicle
VV	Vertical transmit -Vertical receive
VH	Vertical transmit – Horizontal receive
OOB	Out of Bag error
NDVI	Normalized Difference Vegetation Index
AUC	Area Under the receiver operating characteristic Curve
TSS	True Skill Statistic
RF	Random Forest

CHAPTER ONE: INTEGRATION OF RADAR AND OPTICAL SATELLITE DATA FOR FINE SCALE DETECTION OF AN INVASIVE PLANT IN GREAT LAKES COASTAL WETLANDS

Abstract

Great Lakes coastal wetlands have an ecological importance disproportionate to their size, and are extremely vulnerable to invasive plant invasions. Wetland plant invasions can be effectively controlled in their early stages, yet early detection of non-native plants using traditional ground survey methods is time-prohibitive and costly. Remote detection can be effective but challenging due to small population sizes of invasive plants during the early stages of invasion and spatially coarse satellite data. New satellite data sources and analysis techniques offer promise for fine-scale detection of invasive wetland plants using remote sensing. In this study I used a C-band synthetic aperture radar (Sentinel-1) from three different dates with fine-scale multispectral optical imagery (RapidEye) to classify coastal wetland plant communities. I had particular interest in classifying and detecting invasive hybrid cattail (*Typha x. glauca*), which imperils the high quality coastal wetlands of the St. Mary's River. I also compared classification accuracy between Maximum Likelihood and random forest algorithms. Using random forest, I calculated Mean Decrease Accuracy (MDA), which quantifies the relative importance of each variable for the classification. The MDA demonstrated that the early season (May 30th) synthetic aperture radar and the "red-edge", green, and NIR (Near-Infrared) bands of RapidEye were the five most important variables to discriminate

between wetland plant communities. I successfully classified wetland vegetation types at an appropriate scale to guide early detection and management of *Typha x. glauca* invasions into other wetland plant communities. Furthermore, my methods can be used for repeat monitoring of hybrid cattail stands, and can be adapted for remote monitoring in other wetland environments.

Introduction

Wetlands are an ecosystem in peril. In the United States alone, over half of all historic wetlands have been lost since European colonization (Dahl 1990). Activities such as human-mediated dredging, draining, and filling are the major direct contributors to wetland loss and degradation (Gibbs 2016). These losses have important implications for the natural functioning of many ecosystems and of overall biodiversity because wetlands are an essential habitat for many types of wildlife, particularly migratory birds (Junk et al., 2006) and fish (Jude and Pappas 1992). Wetlands also provide humans with a variety of valuable ecosystem services, including improved water quality (Johnston 1991) and flood hazard reduction (Bullock et al., 2003).

Next to direct habitat destruction, invasive plants are considered one of the primary threats to wetland ecosystems. Despite occupying only 6% of the terrestrial and freshwater surface of the earth, wetlands harbor 24% of the world's worst invasive plants (Zedler and Kercher 2004). Invasive plant dominance can impact native wetland plant community diversity and architecture (Houlahan and Findlay 2004), alter sediment nutrient cycling (Templer et al., 1998), modify hydrology (Ayers et al., 2004), and degrade the ecological and societal value of the wetland (Holdredge and Bertness 2011). It has often been demonstrated that early detection and control of invasive plants offers

the best chance of effective management (Rejmánek and Pitcairn 2002). Invasive species also typically have a period of time after initial colonization and before dominance, where individual populations are small and management is most likely (Mehta et al., 2007) Yet, restoration and control efforts often target large, established invasive plant populations, and are often unsuccessful in their management goals (Martin and Blossey 2013; Kettenring and Adams 2011). A major challenge to control is identifying the invasion in its early stages and mapping their spatial extent (Crooks et al., 1999). Because many wetlands are large and relatively inaccessible, field-surveying for invasive plant populations is often not practical or economical.

Remote sensing imagery sources and analysis have increasingly been used to fulfill this management need by allowing for large landscapes to be analyzed, particularly with multispectral satellite imagery (Ozesmi and Bauer, 2002). Despite the potential utility of remote sensing in management, wetlands have historically been challenging in remote sensing efforts because of their unique characteristics (Hestir et al., 2008). In fully terrestrial systems, plants are traditionally differentiated with optical satellite data using their unique spectral signature, particularly their response to near-infrared wavelengths (Lass et al., 2005). By comparison, wetlands have heterogeneous plant communities that result in "mixed pixels," i.e. fine-scale variability in plant composition (Gallant 2015). In addition, there can be a high amount of variability in spectral reflectance within a given species (Adam et al., 2010) and among spectrally similar groups of plant communities (Ozesmi and Bauer 2002). The commonly used Landsat series of satellites provides a spectral and temporal resolution that is often attractive to wetland mappers. However, Landsat has a relatively coarse spatial resolution (30m), which can lead to mapping errors

of smaller landscape units (Ramsey and Laine 1997). Several other imagery sources have been used for wetland remote sensing, each with benefits and limitations with regards to wetlands and invasive plant monitoring. For example, wetland communities have been mapped successfully using traditional aerial photography (Scarpace et al., 1981), hyperspectral imagery (Adam et al., 2010), Light Detection and Ranging (Brock and Purkis 2009), Synthetic Aperture Radar (Bourgeau-Chavez et al., 2001), unmanned aerial vehicles (Jensen et al., 2011), and Terrestrial Laser Scanner systems (Guarnieri et al., 2009). Despite the ability of these data sources to characterize unique aspects of plant phenology, many of these sources can be prohibitively expensive for local management efforts, and may require dedicated technicians.

Two recent satellite products provide an excellent opportunity to improve low cost wetland monitoring, and offer a potentially transformative solution to traditional early detection, which will contribute to control of invasive wetland plants. Sentinel-1, launched in 2014, is a constellation of two satellites that carry a C-band Synthetic Aperture Radar (SAR). SAR is a method of active remote sensing that measures returns from consecutive pulses of microwaves emitted from the sensor to illuminate the Earth's surface. SAR imagery is useful in annual mapping efforts due to its ability to penetrate cloud cover and darkness, which multispectral imagery cannot. Two widely available SAR satellites, ESA ERS-1 and ERS-2 (European Remote-Sensing Satellite), launched in 1991 and 1995, had C-band SAR that aided detection of inundation and biomass in wetlands due to its "double-bounce" effect on emergent vegetation (Bourgeau-Chavez et al., 2001). The now-retired ALOS-1 Phased Array type L-band SAR (PALSAR) multi-temporal (multiple-date) imagery paired with Landsat multispectral imagery has been

used to accurately map wetland vegetation communities (Bourgeau-Chavez et al., 2015). Multi-temporal SAR imagery has previously been used with Landsat imagery to increase the accuracy of wetland mapping due to its ability to detect changes in inundation, phenology, and biomass (Bourgeau-Chavez et al., 2009; Corcoran et al., 2013). However, the 30-meter spatial resolution of Landsat limits its effectiveness for mapping invasive species at a scale to guide early detection and management. In comparison, the use of multi-temporal C-band SAR from the new Sentinel-1 has been relatively unexplored in wetland classification at more regional scales, and may be a complimentary resource when paired with higher resolution multispectral imagery.

The second promising satellite product is RapidEye, a high resolution commercial multispectral satellite constellation launched in 2008 that includes a "red-edge" optical band that has been found to be effective in many measures of plant community delineation (Ramoelo et al., 2012; Hong et al., 2015; Tapsall et al., 2010). RapidEye's 5m resolution allows for relatively low cost, fine-scale mapping. However, RapidEye has been seldom integrated with complementary SAR imagery for fine-scale wetland mapping. A hybrid approach that incorporates both X-band SAR and optical products has previously been used to map wetland communities in great detail (Van Beijma et al., 2014), and RapidEye and Sentinel-1 SAR have been used to classify (categorize) crop types (Lussem et al., 2016). However, RapidEye has never been used with Sentinel-1 C-band SAR to classify wetland plant communities.

Typically, wetlands have been classified with supervised parametric approaches, particularly Maximum Likelihood Estimation (MLE) (Ozesmi and Bauer 2002), a user-friendly technique included in commonly-used spatial analysis and GIS software (e.g.

ArcGIS, ENVI). However, machine-learning algorithms such as random forest (Liaw and Wiener 2002) have become more widespread in remote sensing studies in recent years due to advantages in robustness against overfitting models (Breiman 2001). Another desirable aspect of random forest is its generation of measures of variable importance. Variable importance allows for a more critical examination of which variables (such as imagery sources) are most important for discriminating the vegetation classes of interest. Wetlands have been previously successfully classified with random forest (e.g., Adam et al., 2014; Corcoran et al., 2013), but studies have typically produced coarse vegetation classes within large wetland complexes, rather than finer scale vegetation communities necessary for early detection and management of aquatic invasive plants.

Given the importance of early detection of invasive plants within wetland ecosystems, the main objective of my study was to improve methods to monitor wetlands, and in particular acquire early detection of invasive wetland plant populations and the vegetation communities they impact, using new remote sensing data sources and analysis methods. Emphasis was placed on low cost, high resolution wetland mapping that could be performed annually. I conducted my research in the St Mary's River of Michigan's Upper Peninsula, which represents an ideal study area because of its diverse mix of coastal wetlands and high conservation value. The St Mary's River is of particular interest because of the growing prominence of invasive *Typha x. glauca*, hereafter referred to as hybrid cattail, which is a hybridization of native *Typha latifolia* and exotic *Typha angustifolia* (Smith 1987). Hybrid cattail has a tendency to dominate many wetland plant communities (Frieswyk et al., 2007), having dramatic impacts on plant community richness, litter mass, and nutrient concentration (Tuchman et al., 2009). In

much of my study area, hybrid cattail is still in early stages of colonization, and thus accurate monitoring can guide timely management efforts and detect trends in expansion or contraction over other plant communities. My specific objectives were to compare the effectiveness of imagery source combination models in classifying hybrid cattail and other wetland communities. Once a best model for hybrid cattail and overall wetland accuracy was selected, I aimed to assess the relative importance of C-band SAR and RapidEye optical satellite data variables to suggest better methods for coastal wetland mapping.

Methods

Study Area and Species of Interest

North America's Great Lakes contain 20 percent of the world's surface freshwater by volume and are globally important for biodiversity and ecosystem services (Rothlisberger et al., 2012), with many of these services dependent on Great Lakes coastal wetlands in particular (Prince et al., 1992; Sierszen et al., 2017). Great Lakes coastal wetlands provide habitat for a portion of the life history for 80% of Great Lakes fish species (Jude and Pappas 1992), and are also especially important ecosystems for migratory birds (Riffell et al., 2001). Compared to many of the degraded southern coastal wetlands of Lakes Michigan, Erie, and Ontario, wetlands in Lake Superior and northern Lake Huron are minimally impacted by human disturbance (Cvetkovic and Chow-Fraser 2011). The sole drainage of Lake Superior into the other lakes, and the location of many remaining high-quality coastal wetlands is the St. Mary's River (Fig. 1.1). The St. Mary's River is a large strait that facilitates high shipping traffic, while also supporting large intact wetland systems. While the St. Mary's River supported largely native wetland

communities well into the late 1980's, many formerly diverse plant communities are now dominated by hybrid cattail (*Typha x. glauca*), which has continued to expand via clonal propagation.

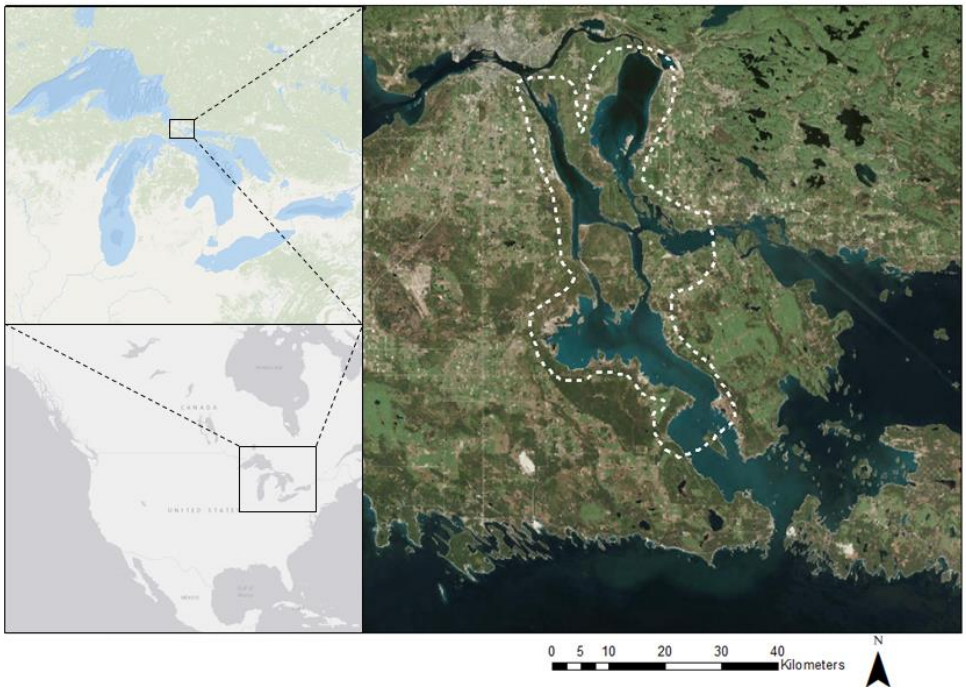

Figure 1.1 Location of the St. Mary's River Study Site in North America's Great Lakes Basin

Hybrid cattail is predominantly an F1 hybrid between native broadleaf cattail (*Typha latifolia*) and exotic narrowleaf cattail (*Typha angustifolia)* which is native to much of Eurasia (Ciotir et al., 2013). The vigorous growth of hybrid cattail has allowed it to thrive in many habitats and accumulate more biomass compared to its parental species (Olson et al., 2009; Bunbury-Blanchette et al., 2015). In Great Lakes coastal wetlands such as those in the St. Mary's River, hybrid cattail has negative effects on native plant biodiversity and community structure (Mitchell et al., 2011). To control hybrid cattail, treatment efforts must focus on small or recently established populations, as certain

harvest methods have proven effective in removing hybrid cattail and increasing native plant diversity (Lishawa et al., 2015). Remote sensing based monitoring and detection methods are superior to traditional land-based surveys in efficiently detecting these populations, as they can cover a larger area more economically and identify inconspicuous or inaccessible invasive plant populations.

Remote wetland classification in the Great Lakes has typically focused on detection of *Phragmites australis,* an invasive plant structurally similar to hybrid cattail that outcompetes native wetland vegetation in many areas of the Great Lakes. However, few mapping efforts have focused on examining the fine scale dynamics of hybrid cattail, one of the principal invasive plants in the high-quality coastal wetlands of Michigan's Upper Peninsula. To address the need for finer scale hybrid cattail monitoring and wetland management, maps must be produced at a more detailed scale to detect the dynamics of smaller populations, and do so at a low cost. In particular, avenues where freely available and/or low-cost imagery are desirable, as they reflect the realities of budget constraints in natural resource and management organizations.

The study was conducted on a 721 sq. km area of the St. Mary's river, containing much of the coastal wetlands along the waterway and representing a wide range of wetland plant communities. Previous maps of Great Lakes coastal wetlands focus on basin-wide trends in plant communities (Bourgeau-Chavez et al., 2015). However, many of the Cooperative Invasive Species Management Areas, and other independent management units in the Great Lakes operate and are funded at more regional operational scales.

Field Data

Field data for a reference dataset were gathered from the Sault Tribe of Chippewa Indian's Inland Fish and Wildlife Department during summer 2016. Plant surveys consisted of an individual or team walking 300 meter transects along a wetland, and having a surveyor estimate cover percentages of different plant species in a one meter quadrat at 25 meter intervals (for a total of 13 quadrats sampled per transect). 25 transects were surveyed throughout the western extent of the study site, with a total of 325 reference quadrats (Fig. 1.2). Overhead photos were taken one meter above the vegetation canopy at each quadrat in 19 of the 25 transects using a digital camera attached to a pole, with the photo absences occurring in transects located in terrain that made maneuvering the photo pole difficult. Photos were used to validate surveyor species identification.

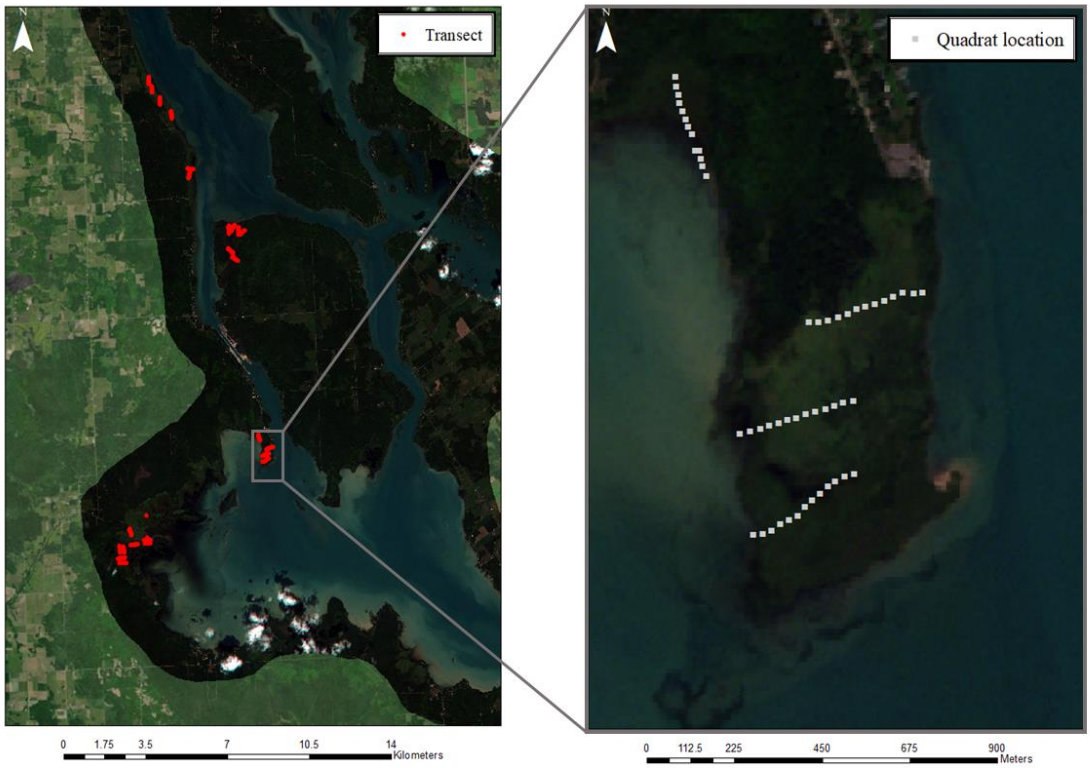

Figure 1.2 Configuration of Transect Locations in the Study Site (Left) and Quadrat Points at Each 25 Meter Interval (Right)

A total of 11 vegetation classes were established by differences in plant communities, considering physical structure, species composition, and water depth. These included 1) hybrid cattail, 2) mixed sedge, 3) open bulrush, 4) emergent/floating, 5) wet grass meadow, 6) floating leaf, 7) wet shrub, 8) dry shrub, 9) field, 10) forest, and 11) open water.

Reference data to train the models were derived from two sources, directly from the survey points along transects (or spaced along transects between reference sites of the same class), and indirectly based on interpretation of high resolution aerial (NAIP) and UAV imagery taken in summer 2016. UAV imagery was captured by a senseFly eBee, a

fully autonomous UAV system to produce multispectral imagery in four bands at five centimeter resolution. Some classes, such as hybrid cattail, mixed sedge, wet shrub, and dry shrub, had pixels largely derived from reference quadrats due to their inconspicuous spectral characteristics when observing aerial imagery. The other classes, open bulrush, emergent/floating, wet grass meadow, floating leaf, field, forest, and open water, were distinct enough in the imagery sources to create reference pixels largely independent from reference quadrats, and were spread out within the study area. A total of 1041 five meter reference pixels were created from these two methods, which were randomly partitioned into training and testing subsets (Fig. 1.3), with a minimum of 72 reference pixels assigned to a class (Table 1.1)

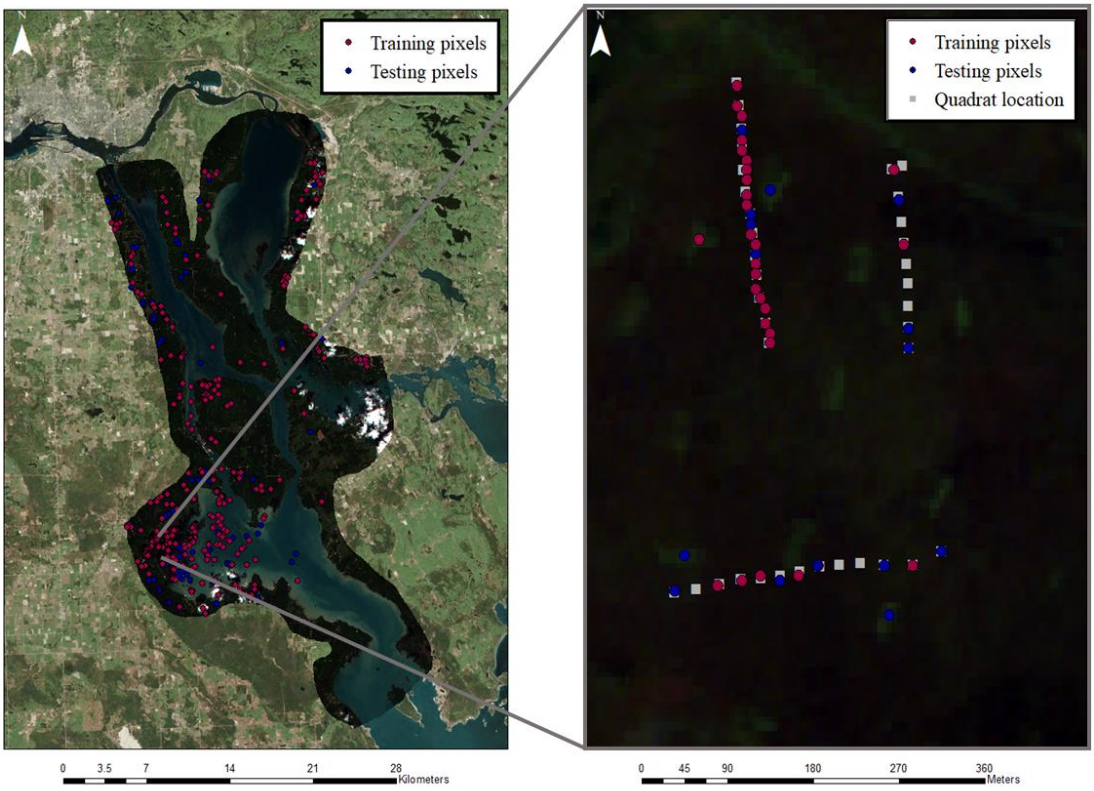

Figure 1.3 Pixel Locations For All Classes in the Study Site, Partitioned Into Training (Red) and Testing (Blue) Sets (Left), and Example of Pixels Assigned to Reference Quadrats (Right)

Table 1.1 Description of Wetland Community Vegetation Classes and Total Number of Reference Pixels in Each Class

Name	Acronym	Major Genera	Number of Reference Pixels
Hybrid cattail	HC	*Typha*	101
Mixed sedge	MS	*Carex, Schoenoplectus*	117
Open bulrush	OB	*Schoenoplectus*	103
Emergent/floating	EF	*Schoenoplectus/Nymphaea*	80
Wet grass meadow	WG	*Calamagrostis/Phalaris*	115
Floating leaf	FL	*Nymphaea/Nuphar/Potamogeton*	76
Wet shrub	WS	*Myrica/Salix*	74
Dry shrub	DS	*Cornus/Salix*	72
Field	FD	Various	101
Forest	FS	Various	100
Open water	OW	N/A	102

Satellite Data and Processing

A cloud free RapidEye image of 721 sq. km was captured on August 29th, 2016 and delivered as an orthorectified product. RapidEye imagery is provided as orthorectified, multispectral data from a five-satellite constellation. The multispectral image contains five bands, each with a pixel size of five meters: blue (440-550nm), green (520-590nm), red (630-685nm), red-edge (630-685nm), and near-infrared (760-850nm).

I accessed SAR imagery from Vertex, a data portal operated by the Alaska Satellite Facility (Copernicus Sentinel data 2016. Retrieved from ASF DAAC 18 December 2016, processed by ESA). Interferometric-Wide, Ascending Sentinel-1 SAR scenes in May, July, and August were included to capture the entire growing season of these plant communities before senescence. SAR data was processed using the Sentinel Application Platform (SNAP), with each SAR image (10 by 10 meter pixel spacing) subset to the study area and processed with thermal noise removal, radiometric calibration to sigma0, speckle filtering, and range-doppler terrain correction using a median filter (see Moreira et al., 2013) for details on the processing and calibration techniques). The C-band SAR imagery used in this study is available in two polarizations: VV (Vertical-transmit Vertical-receive) and VH (Vertical-transmit Horizontal-receive). Fig. 1.4 is an example of the RapidEye optical imagery compared to VH and VV SAR multi-date composites and their respective vegetation communities within the scene.

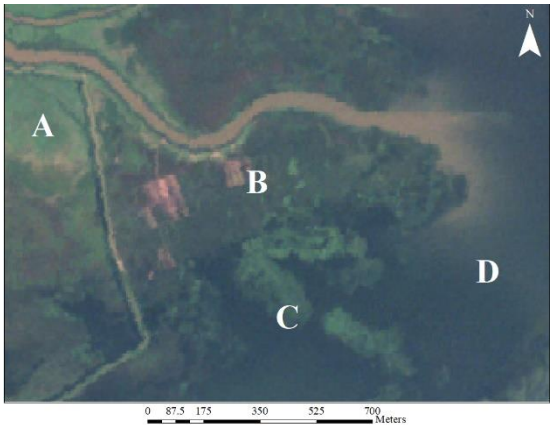

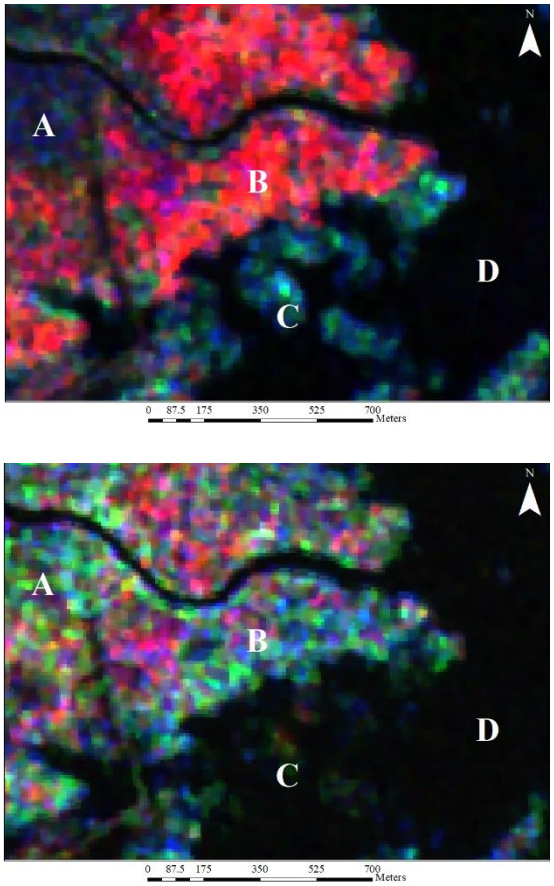

Figure 1.4 Optical RapidEye (Top) Multi-Date Sentinel-1 VV SAR (Inundation) (Middle) Multi-Date Sentinel-1 VH SAR (Biomass). In Each Image, Labeled Examples of Wet Grass Meadow (A), Hybrid Cattail (B), Open Bulrush (C), and Open Water (D). Note Differences in Characterization of B) (Hybrid Cattail) and A) (Wet Grass Meadow) Between the VV SAR and VH SAR Images

The six bands of SAR were resampled from their native resolution of 10 meters using bilinear interpolation to a working resolution of 5 meters in order to match the resolution of the RapidEye imagery. The resampled SAR and the five bands of RapidEye optical imagery were stacked into a composite, 11 band image. The values of these 11 bands across the study area were subset to the pixel locations in our reference dataset, and exported to testing and training datasets.

Classifications and Accuracy Assessment

Random Forest

Random forest is an ensemble learning method of supervised nonparametric classification that generates decision trees, and predicts one of the specified classes based on a majority vote (Liaw and Wiener 2002). The random forest classification was performed using the "randomForest" package in R (Liaw and Wiener 2014) and imputed to output a spatial product based on the predictors generated (Crookston and Finley 2008). Random forest was chosen because of its accuracy in land-cover classifications (Rodriguez-Galiano et al., 2012) and its ability to determine a ranking of variable importance. For the random forest models in this study, 500 decision trees were used, based on stabilization OOB error rate after this default number. The only parameter edited by the user in a random forest, other than the number of decision trees, was the number of parameters randomly sampled at each node. This value was set as 3 after iterative runs the model showed no decrease in accuracy with higher values. Cross validation is sometimes considered unnecessary in random forest models (Breiman 1999), as the random forest by default sets aside 2/3 of the data for training and the remaining 1/3 for testing for an Out of Bag (OOB) error. This approach typically reduces the need for an independent validation set, but because of the need to compare the random forest to the Maximum Likelihood Estimation, reference pixels were randomly partitioned into training (70% of reference pixels) and testing (30% of reference pixels) datasets, to cross-validate each algorithm generated on the training dataset with the testing dataset. Variable importance was determined in the random forest by randomly permuting the OOB samples for each predictor and subtracting the predictor specific

OOB performance from the whole-model OOB accuracy. This calculation produced a Mean Decrease in Accuracy (MDA) on which to rank the variables from most to least important in the creation of the decision trees, and thus their importance to the models (Liaw and Wiener, 2014). The relative ranking of these variables to each other was considered a more important measure than the magnitude of their values.

Maximum Likelihood Estimation

Maximum Likelihood Estimation (MLE) is a supervised parametric classification method whereby the maximum likelihood of a pixel belonging to a class is determined by parametric rules established by the training pixels. MLE was chosen due to its ease of use, common presence in geospatial software, and legacy use in land use classifications. Although MLE classifications are considered somewhat out of date in comparison to modern machine learning classifications, the process is more user-friendly in non-expert settings. The training (70%) and testing (30%) pixels came from the same dataset established for the random forest models, and were used to generate class and overall accuracy for the MLE.

Model Creation

To assess the contribution of optical and SAR imagery, I created four random forest models with differing band combinations out of my 11 variables (5 optical and 6 SAR) (Table 1.2). I performed five different classifications based on different combinations of input variables (i.e. image bands) and classification methods. Models included a full input MLE, and four random forest models. Random forest models included an optical-only, SAR-only, single-date SAR, and full-input model to determine

how different imagery combinations impacted class and overall accuracies. An overview of processing and analysis workflow is provided in Fig. 1.5.

Table 1.2 Input Variable Combinations in RF and MLE Models. "X" Denotes Inclusion of Variable Into Each Model

Input Variable	RF Model				MLE
	RF1	RF2	RF3	RF4	
RapidEye blue band	X		X	X	X
RapidEye green band	X		X	X	X
RapidEye red band	X		X	X	X
RapidEye red edge band	X		X	X	X
RapidEye NIR band	X		X	X	X
August 22 VV SAR		X	X	X	X
July 17 VV SAR		X		X	X
May 30 VV SAR		X		X	X
August 22 VH SAR		X	X	X	X
July 17 VH SAR		X		X	X
May 30 VH SAR		X		X	X

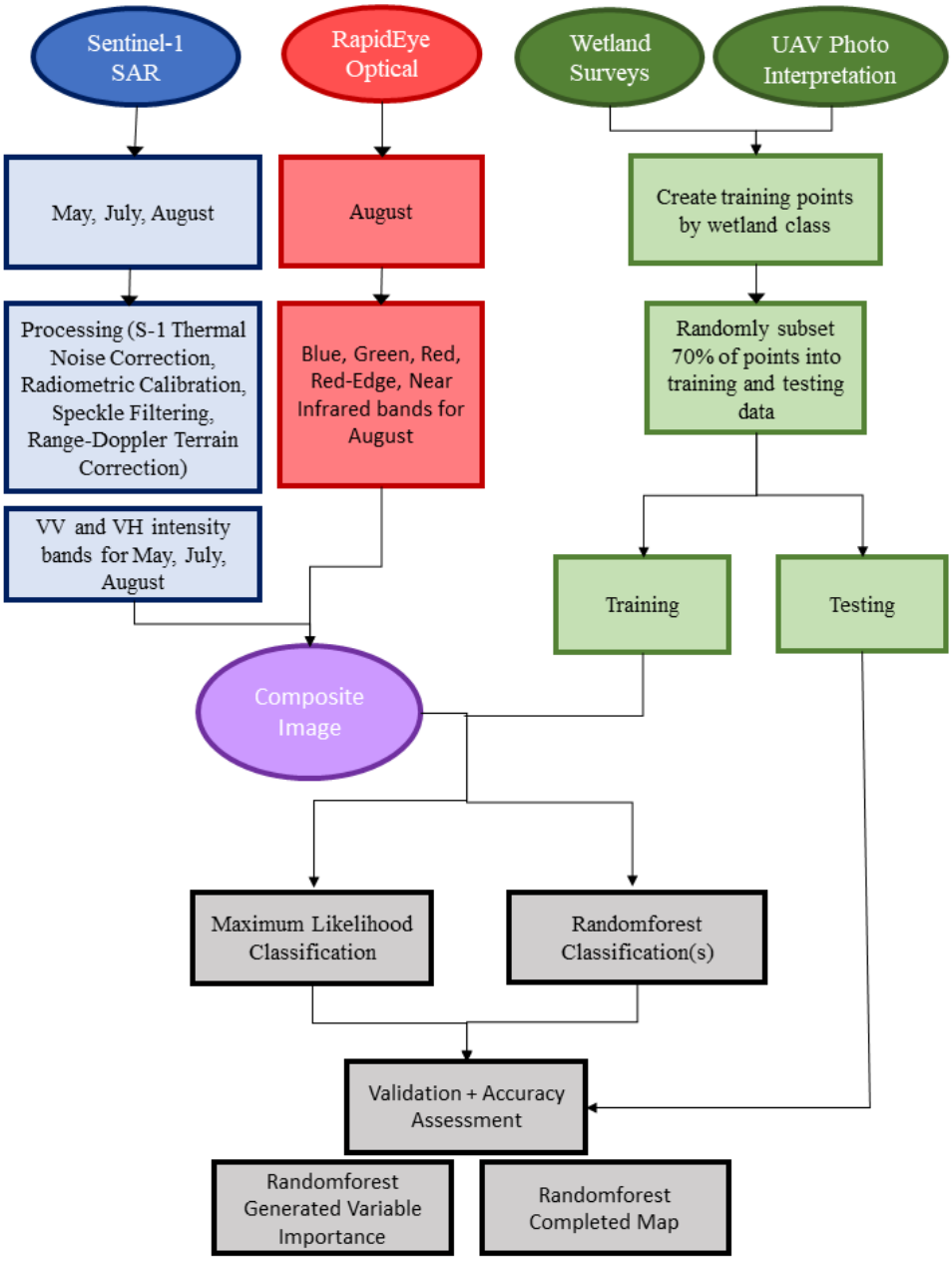

Figure 1.5 Processing workflow of RapidEye and SAR Imagery for Classification and Analysis

Results

Comparison of MLE and Random Forest Models

Overall Model Comparison

Out of the five total models tested (Table 1.3), the full-input random forest model (RF4) had the highest overall accuracy. The optical-only (RF1) and SAR-only (RF2) classifications were of similar overall accuracy, but the inclusion of the peak-phenology August VV and VH SAR data into the optical classification (RF3) resulted in an increase of 6.5% overall accuracy. While the MLE model used the same variables and reference data as the RF4, it was 4.9% less accurate overall. Full error matrices for all five models can be found in Appendices A.1.1:A.1.5.

Table 1.3 Overall Classification Accuracy (Percentage of the Total Number of Testing Pixels Correctly Classified by the Training Classification) of All Models

Model	Overall accuracy (%)	kappa Coefficient
RF1	80.52	0.78
RF2	78.57	0.76
RF3	87.01	0.86
RF4	90.26	0.89
MLE	85.39	0.84

Hybrid Cattail Classification Accuracy

Results for model hybrid cattail accuracy differed from model overall accuracy (Table 1.4). The full-input random forest model (RF4) and the full-input MLE model (MLE) shared the top ranking with an identical hybrid cattail producer's accuracy (Table 1.4). Notably, the SAR-only model (RF2), had a high hybrid cattail producer's accuracy that was identical to the single-SAR date combination model (RF3), and surpassed the accuracy of the optical-only model (RF1).

Table 1.4 Producer's Accuracy of Hybrid Cattail Class in Each Model

Model	Description	HC Accuracy (%)
RF1	Optical-only	80.00
RF2	SAR-only	86.67
RF3	Single-date SAR	86.67
RF4	Full-input	90.00
MLE	Full-input MLE	90.00

Random Forest and Maximum Likelihood Individual Wetland Class Comparisons

Because the full-input random forest model shared identical variable inputs to the MLE, comparisons of algorithm impacts could be made. Class producer's accuracy differences between the RF4 and MLE models (Table 1.5) ranged from 0-11.4%, with the largest difference found in mixed sedge, and identical accuracies in hybrid cattail and

floating leaf classes. Differences in accuracies between the two algorithms tended to favor the RF4, except in the case of the wet and dry shrub classes.

Table 1.5 RF4 and MLE Producer's Accuracies of Each Vegetation Class

Vegetation Class	RF4 Accuracy (%)	MLE Accuracy (%)	Difference (%)
Hybrid cattail	90.00	90.00	0.00
Mixed sedge	91.43	80.00	11.43
Open bulrush	100.00	93.33	6.67
Emergent/floating	95.83	87.50	8.33
Wet grass meadow	94.11	91.17	2.94
Floating leaf	86.36	86.36	0.00
Wet shrub	68.18	72.72	-4.54
Dry shrub	80.95	85.71	-4.76
Field	96.67	86.67	10.00
Forest	80.00	70.00	10.00
Open water	100.00	93.33	6.67
Mean class accuracy (%)	89.41	85.16	

Importance of SAR and RapidEye Variable Contribution to Classification Accuracy

Because the full-input random forest model (RF4) proved to be the most accurate model between overall and hybrid cattail accuracy, and contained all of the variables used in this study, it was used for further analysis of variable importance. I first calculated the Mean Decrease in Accuracy (MDA) which estimates a decrease in model accuracy when the individual variable is excluded. The ranking of all variables by MDA in the RF4 model (Fig.1.6) indicated the top five variables consisted of three optical and two SAR bands. In particular, both polarizations (VV and VH) of May 30th SAR were highly ranked compared to the July and August SAR dates.

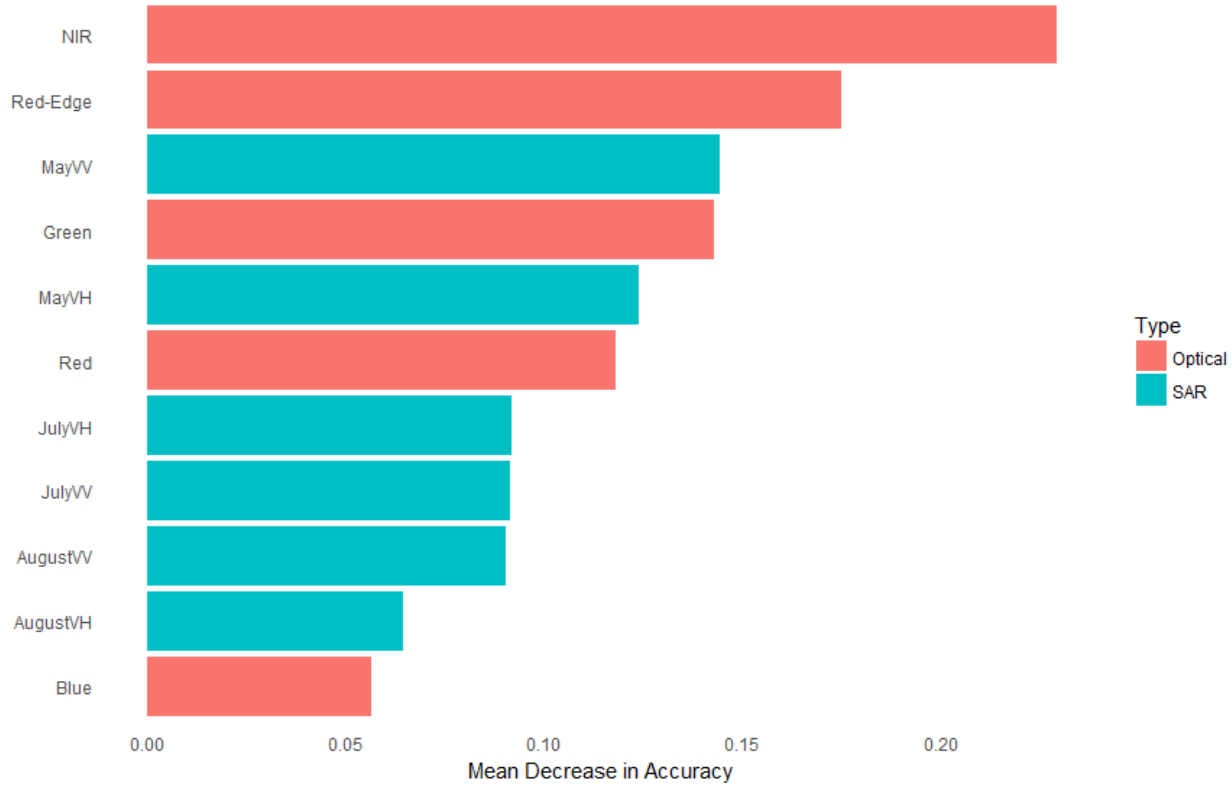

Figure 1.6 Mean Decrease in Accuracy (MDA) Measure of Variable Importance in the Full Input Random Forest Model (RF4). In descending order of importance, RapidEye NIR band (NIR), RapidEye red-edge band (Red-Edge), May 30 VV SAR (MayVV) RapidEye green band (Green), May 30 VH SAR (MayVH), RapidEye red band (Red), July 17 VH SAR (JulyVH), July 17 VV SAR (JulyVV), August 22 VV SAR (AugustVV), August 22 VH SAR (AugustVH), and RapidEye blue band (Blue).

When the RF4 classification of the study area was mapped (Fig. 1.7), it classified several circular colonies of hybrid cattail around 50 meters in diameter in Munuscong Bay region. In an area known as the Munuscong State Wildlife Management Area, some of these colonies occur in large, native mixed sedge areas. Large artefacts are usually where a single date of SAR measured a large moving object, such as large ships or planes.

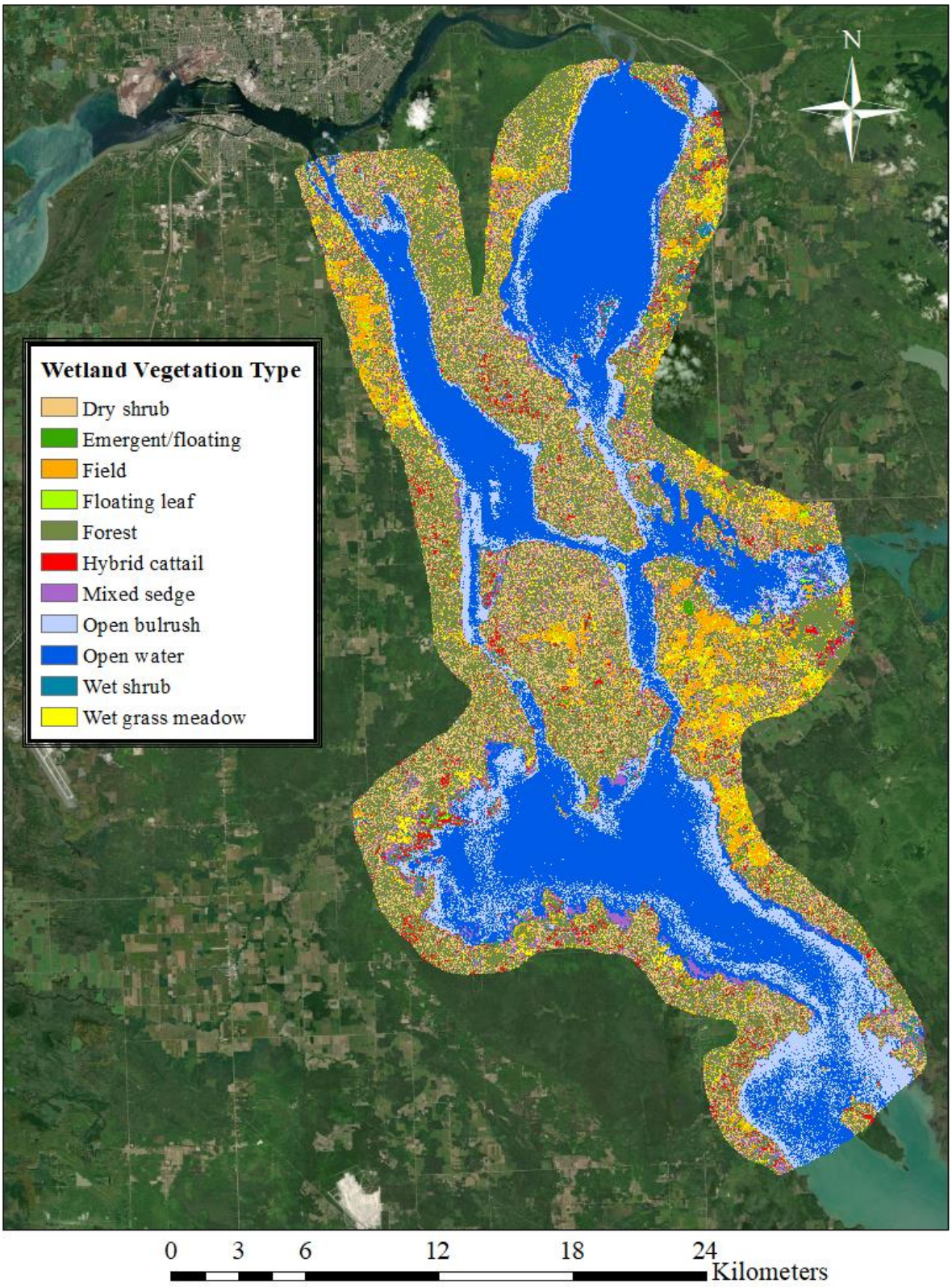

Figure 1.7 Vegetation Community Classification Map of the Full-Input Random Forest Model (RF4) in the St. Mary's River

Discussion

Classification Accuracies and Spatial Autocorrelation

The full-input random forest model (RF4) was superior in overall classification accuracy to the MLE with identical full inputs (Table 1.5). This consistent with similar studies comparing MLE to machine learning techniques such as random forest and Support Vector Machines in crop delineations (Lussem et al., 2016; Nitze et al., 2012). When field data are extensive, such as in this study, random forest may perform better than an MLE, as a strength of the method lies in dealing with unbalanced or missing data (Cutler et al., 2007). In my study, training pixels were either selected on or adjacent to reference quadrats, or selected from high-resolution imagery if the class could be easily discerned. While utilization of one meter quadrats is typical of Great Lakes coastal wetland monitoring (Uzarski et al., 2017), scalability with the satellite imagery (5 and 10 meters), and a lack of data across the extent of the study area (Fig. 1.2) may have resulted in spatial autocorrelation and inflated class accuracies. While spatial autocorrelation is an inherent element of natural physical systems (Legendre 1993), it should be considered when interpreting the validity of mapped classifications in areas where our data were poor, particularly the eastern extents of the river.

Importance of Optical and SAR Variables

By combining both SAR and optical imagery sources, classifications reached their highest accuracy in classifying hybrid cattail and other wetland communities than with either source of imagery used alone. SAR variables, in particular the May VV SAR, were some of the most important variables (Fig. 1.6). May SAR among the three dates may have been important due to the characteristics of emerging marsh vegetation in the

spring, before peak phenology later in August. July at a similar latitude in the Mer Bleue Bog in Ottawa, Canada (Baghdadi et al., 2001). The importance of the May VV SAR, which ranked among the top 3 variables, was likely due to its measurement of emerging vegetation in inundated areas, which encourages specular reflection off of a water surface and again off vertical vegetation, resulting in strong backscatter (Bourgeau-Chavez et al., 2009). In comparison, VH SAR is commonly utilized to measure biomass, especially in woody or terrestrial environments (Martinez and Le Toan 2007). Outside of May, SAR was not among the top 5 ranked variables, which may indicate a lack of ability to penetrate peak phenology canopies in the later season. Although HH (Horizontal-transfer Horizontal-return) polarization C-band SAR has been found to be superior to VV in some wetland classification efforts (Lang et al., 2008), and is offered as a Sentinel-1 product, it was unavailable for this region of the Great Lakes during the time of this study.

The red-edge band that makes RapidEye a unique product from other multispectral sensors was among the most important variables in the full-input random forest model, and has been a commonly used indicator of plant vigor and other physical qualities due to the small amount of absorption and high amount of reflectance in plant leaves (Filella and Penuelas 1994; Delegido et al., 2011). Red-edge was ranked second in its MDA among the 11 variables only to the near-infrared band. Near infrared is similar to red-edge in that it is typically found to have a high reflectance value in healthy plants, with differences found due to plant structure, leaf chemistry, and disease (Knipling 1970).

In the combination of SAR and optical variables, qualities that may be missed by one type of imagery can be captured by the other. Wetland communities with similar

optical properties may have different polarimetric or structural properties that can be captured by the SAR imagery but missed in optical bands due to dense canopies, and optical bands may capture information about stress or senescence that may be lost in SAR backscatter. (Silva et al. 2008; Hess et al., 2003). In the present study, a combination of both in the single-SAR date combination (RF3) and the full-input random forest model (RF4) resulted in the highest overall accuracies for wetland classes (Table 1.3).

Invasive Species Management Implications

The combination of fine resolution optical and SAR data resulted in maps that detected small (50 meter) colonies of hybrid cattail in a wetland landscape, which would have likely mixed into pixels of coarser datasets such as Landsat (30 meters). In my best classification, I was able to map hybrid cattail with 90.00% producer's accuracy (100% - omission error) (Table 1.3) and 90.00% user's accuracy (100% - commission error). In land use classifications, simply stating an overall accuracy can be problematic for management interpretation. Both the perspective of the map user and map maker must be considered. For a surveyor in areas mapped as hybrid cattail for ground-truthing or management, a high user's accuracy will signify that most pixels on the map are the plant population they claim to be on the ground. For a user creating hybrid cattail maps based on reference data, producer's accuracy may be a more important consideration, as it signifies an agreement between the vegetation class of the reference plots and the newly created map. Considering that each type of accuracy provides different information, a focus on one may provide a misleading sense of accuracy that may compromise proper inference needed for management decisions. Creation of accurate maps to detect new

populations must consider both, so the map is seen as a worthy resource by the surveyor and in agreement with reference data by the map-maker.

New detections of small patches of hybrid cattail offer an opportunity to remove or halt hybrid cattail expansion into native wet meadows and emergent marsh. Previous studies have found success in treating small patches of hybrid cattail with below-water harvesting techniques, ultimately resulting in decreases of hybrid cattail cover and increases in native vegetation recruitment (Lishawa et al., 2017). These methods also allows for more effective post treatment documentation of management outcomes without requiring detailed on the ground surveys in subsequent years following management actions. Additional studies of long term mapping are recommended to test the utility of detection of new or expanding populations of hybrid cattail over time.

Annual Monitoring Recommendations

Based on the results of this study and the maps I were able to generate, I recommend an approach for annual mapping of hybrid cattail and other wetland communities that incorporates a single optical scene with multiple SAR scenes throughout the growing season. Although many studies use multi-temporal RapidEye, the minimum cost to acquire imagery can run in the thousands of dollars, which can represent a significant investment for a regionalized management unit. SAR also has the benefit of detection ability under cloudy conditions that may severely limit or eliminate the viability of other imagery sources on a reliable basis necessary for dense time series analysis of multispectral imagery. In comparing strengths of MLE and random forest, random forest may be more flexible to the caveats that most regional management efforts face in terms of the quantity and quality of training data and validation datasets needed.

Random forest also gives an easy to conceptualize measure of variable importance, which may be beneficial for determining the usefulness of paid imagery sources to freely available ones and decreasing total computing effort. A downside to random forest is that it requires more knowledge of coding compared to MLE, which is a native function of common software such as ArcMap.

For other invasive species that may not require the fine scale resolution of RapidEye, a combination of multi-temporal ESA Sentinel-1 SAR and Sentinel-2 optical imagery using the methods and variables outlined in this study may be ideal. While Sentinel-2 bands (10 meters RGB and NIR, 20 meters for red-edge) have a slightly lower spatial resolution than RapidEye (5 meters), the 14-day return time and free access makes it a worthy resource for future exploration in invasive plant detection and mapping in wetlands. Because these methods were designed for use by smaller scale natural resource management units, localized knowledge and a base understanding of image interpretation is critical to recruit such knowledge for classification supervision and the creation of helpful spatial products and analysis.

Conclusions

Meeting the challenge of detection of fine-scale vegetation dynamics and invasions is now possible with widespread imagery and techniques. The primary goal of this study was to highlight methods that produce reliable, ecologically relevant spatial data for the use of regional natural resource managers, with a focus on hybrid cattail. Mapping of hybrid cattail extent allows for more efficient and strategic management when maps are produced in annual series. I found that of RapidEye optical and Sentinel-1 SAR imagery complement each other well in the classification of wetland communities in

the St. Mary's River, and their dual use could have high transferability to invasive wetland plants and wetland landscapes in other regions. A random forest model with all optical and SAR variables allowed for the highest classification accuracy when compared to other combinations and the Maximum Likelihood Estimation. Through random forest, I also found that the optical and SAR variables co-dominated as the most important variables, as each had two representatives in the top 4 ranked variables.

Worldwide, wetland habitats suffer destruction from development and the introduction of invasive species. When accurate, ecologically relevant maps and other spatial products are able to be created in widespread practice, resources and policy can be more efficiently directed to put those systems on a positive trajectory. The proliferation of these tools and methods will ultimately aid in immediate and long-term conservation plans to protect, maintain, and restore natural communities.

CHAPTER TWO: USE OF LIDAR AND RADAR DERIVED VEGETATION METRICS TO PREDICT THE SPREAD OF AN INCONSPICUOUS INVASIVE WETLAND PLANT

Abstract

Remote sensing has seen increased use as a resource for invasive plant mapping as data sources and processing methods become more abundant and accessible. Many animal habitat suitability studies have shown the usefulness of fine-scale, remote-sensing derived metrics for species-specific habitat requirements. In this study, I used fine scale elevation and habitat structure derived from lidar and Synthetic Aperture Radar to help predict the habitat suitability of an inconspicuous wetland invasive plant, European Frogbit (*Hydrocharis morsus-ranae*), in Munuscong Bay, Michigan, USA. Lidar-derived elevation was the most important covariate to predict frogbit habitat suitability, although biotic variables such as NDVI (Normalized Difference Vegetation Index), lidar-derived vegetation cover, and radar-derived marsh inundation change also contributed. These biotic variables decreased predicted habitat area where elevation detected the water surface level to be, detecting suitable habitat provided by sufficiently dense emergent wetlands. From the relationship between frogbit and lidar-derived vegetation cover, I determined that frogbit likely invades marsh sites with sufficient emergent vegetation density to protect from wave energy disturbance, but with sufficient light to recruit annual turions. A map of the potential frogbit habitat indicates that Munuscong Bay has several areas of suitable wetland for it to expand to, and continued expansion appears to

be largely limited by wave energy and dispersal constraints. Use of fine-scale habitat covariates determined from lidar and radar should see wider use in species distribution modeling to create better predictions of invasive plant expansions.

Introduction

Invasive species are a cause of dramatic change in ecosystem functionality and biodiversity from local to global scales (Molnar et al., 2008; Vitousek et al., 1997; Mack et al., 2000). In the United States alone, the economic losses attributed to invasive species have been valued at up to $120 billion per year (Pimentel et al., 2005). Biological invasions, once established, have played a major part in extinctions of native species across the globe, driving biological homogenization across ecoregions (Clavero and García 2005; Olden et al., 2004). Invasive plants in particular are known to have the potential to cause ecosystem level impacts such as changes in carbon and nitrogen cycles (Liao et al., 2006; Vitousek 1987), hybridization with similar native species (Ellstrand and Schierenbeck 2000), and outcompeting native plants (Hejda and Py 2009). Despite this risk, resources to combat invasive species are not often allocated optimally, and restoration and control efforts often fail management goals (Martin and Blossey 2013; Kettenring and Adams 2011; Leung et al., 2002). Optimal funding allocation to invasive species surveillance and management could therefore benefit from predictive models that incorporate a comprehensive risk analysis framework (Lodge et al., 2016). Such predictions of invasive populations may be most effective when identifying areas in the landscape where populations may be at a smaller extent, posing a more economically feasible target (Crooks et al., 1999). A study of invasive species have similarly found

prediction guided prevention to be a rational economic solution in a cost-benefit analysis (e.g., Keller et al., 2008).

Species distribution models (SDMs) have been operationalized as a predictive resource that typically combine occurrence records of a species with environmental covariates to estimate their potential distribution across a landscape (Elith and Leathwick 2009). They can be applied as a valuable risk analysis resource in invasive plant management by predicting the area where a species invasion is most likely to occur, refining surveillance efforts in the search area (Crall et al., 2013; Jiménez-Valverde et al., 2011; Underwood et al., 2004; Villero et al., 2017). One of the earliest SDMs, BIOCLIM (Beaumont et al., 2005), focused on estimating the potential spread of invasive species through 35 biologically relevant climatic covariates. These covariates see continued use in continental scale estimates of invasive plant distribution, particularly in the context of species response to different projected climate change scenarios (Booth et al., 2014). However, due to the coarse spatial scale at which these abiotic climatic covariates are produced (1 km^2) there has been criticism regarding the ability of these models to account for finer scale complexities in species interactions and dispersal patterns (Pearson and Dawson 2003). The integration of biotic interactions has been explored as technology allows for more spatially explicit covariates that can improve model performance (Wisz et al., 2013). In addition, subsequent inconsistencies have been found when comparing coarse and fine scale environmental variables, with serious implications of fine-scale habitat change being lost with models built incorporating coarser climate covariates (Franklin et al., 2013). As SDMs become more popular in conservation and management efforts, spatially explicit environmental covariates that better represent the scale that key

ecological processes occur at are needed to improve model inference (Guisan and Thuiller 2005).

Remote sensing datasets allow for physical attributes of large landscapes to be analyzed, measuring a wide variety of environmental characteristics in an area and how those characteristics may change over time. The ability to utilize these measurements as metrics for covariates in SDMs has been noted (Kerr and Ostrovsky 2003), but the use of remote sensing data to provide covariates for biological relationships remains uncommon. Some studies have highlighted a need for the inclusion of more advanced remote sensing data, such as lidar, radar, and hyperspectral imagery metrics as covariates to characterize species habitat use (e.g., Ficetola et al., 2014; Rocchini et al., 2015; He et al., 2011). In particular, novel covariates characterizing habitat structure sourced from lidar and radar-derived metrics are uncommon in SDM literature despite their widespread use in remote sensing studies. Compared to often-used vegetation indices (e.g., NDVI), which measure plant productivity and leaf chemistry (Pettorelli et al., 2005), lidar and synthetic aperture radar (SAR) measure unique structural characteristics that may improve the performance of SDMs. Lidar sensors are an active method of remote sensing that can measure the three-dimensional structure of plant communities, providing estimates for vegetation height, cover, and heterogeneity (Cohen et al., 2002). While lidar has been used to characterize habitat in terms of animal-plant interactions (Valle et al., 2011; Ficetola et al., 2014; Vierling et al., 2013; Jones et al., 2010; Vierling et al., 2008), metrics describing three-dimensional plant architecture have not been utilized as a proxy for plant-plant interactions to improve SDM predictions of invasive plant habitat and distribution. SAR is another method of active remote sensing that has commonly been

used in ecological contexts to measure characteristics of emergent vegetation and soil moisture (Lang et al., 2008) and forest biomass (Carreiras et al., 2013; Koch 2010). However, SAR has been seldom examined as a source for covariates in SDM's, despite the potential to create habitat covariates from backscatter intensity measurements (Saatchi et al., 2008; Buermann et al., 2008).

While remote sensing data are often used to detect the current extent of canopy-dominating invasive plants, challenges remain in the direct detection of inconspicuous, understory invasive species. One approach that can be used in these instances is to model the habitat suitability of a below-canopy invasive plant using remote sensing derived ecologically meaningful habitat covariates derived by remote sensing. This approach also addresses some of the criticisms of continuous remote sensing derived covariates in plant SDMs, as they may measure the characteristics of the plant directly instead of its habitat, leading to the prediction of current rather than potential extent in canopy-dominant invasive plants (Bradley et al., 2012). Knowledge of the biological interactions of invasive plants with other species, how they may limit or promote establishment, and how they may be measured using remote sensing have previously resulted in successful extent mapping of inconspicuous below-canopy invasive plants (Joshi et al., 2006). However, these principles have not seen widespread use in inconspicuous invasive plant SDMs.

The objective of this study was to improve the performance of an inconspicuous invasive plant SDM using lidar and SAR derived metrics that serve as proxies for species-specific habitat requirements. I used these covariates to map the potential distribution of the inconspicuous invasive wetland plant, *Hydrocharis morsus-ranae*

(European frogbit) in a freshwater coastal wetland complex in the Great Lakes Basin. In Great Lakes coastal wetlands, frogbit extent is limited by wave energy, leading to a strong understory association with emergent herbaceous wetland species such as fellow invasive *Typha x. glauca*, hereafter referred to as hybrid cattail (Lishawa, MISGP 2015). Because the vertical and above water structure of hybrid cattail can differ depending on age and water depth (Mitchell et al., 2011; Price et al., 2014), a superficially homogenous stand can represent a heterogeneous landscape of varying light availability and vertical structure. To measure the biological interactions between inconspicuous frogbit and conspicuous emergent wetland communities in a predictive SDM, I used topobathymetric lidar made available through NOAA's Digital Coast data platform, ESA Sentinel-1 Synthetic Aperture Radar (SAR), RapidEye multispectral imagery, and occurrence records through fieldwork and online databases. To my knowledge, this is the first time vegetation measurements from lidar and radar have been purposed to generate ecologically meaningful habitat characterizations in invasive plant distribution models. In particular, I was interested in testing two questions: Which lidar, radar, and multispectral-derived biotic covariates are important in predicting frogbit habitat suitability, and how do their predictions compare to those made with only abiotic elevational data? And, how does frogbit habitat suitability change based on a gradient of lidar-derived marsh architecture?

Methods

Species and Study Area

European Frogbit (hereafter frogbit) is an aquatic floating macrophyte of the family Hydrocharitaceae, native to Eurasian and North African wetlands and waterways.

In North America, frogbit has spread rapidly via vegetative growth and turions (overwintering buds) into ponds, canals, ditches, wetlands, and other areas with slow moving water (Catling and Dore 1982). First introduced in Canada as an ornamental garden plant in 1932 from a population in Zurich, Switzerland, it has spread from Ontario and the St. Lawrence River to the Great Lakes region (Zhu et al., 2018). When located in suitable habitat, frogbit creates floating mats of interlocking ramets, resulting in reduced native submerged plant diversity, clogged irrigation flows, and restricted water traffic (Catling et al., 2003; Eppers et al., 2008). However, Halpern et al., (2017) found that frogbit coverage, individual plant phenology, and propagule pressure varied depending on the vegetation characteristics of the wetland community it occurs within. Although there is a gap in experimental studies of the effects of frogbit in wetland communities, similar well studied invasive floating plants such as water hyacinth (*Eichhornia crassipes*), have found context-dependent impacts on invaded ecosystems at each invaded site (Villamagna and Murphy 2010).

My study area was the coastal wetlands of Munuscong Bay (46.20°N, -84.16°W) in the St. Mary's River, MI, USA (Fig. 2.1). The St. Mary's River connects Lake Superior to Lake Huron, and serves as a transportation link for shipping routes in the Great Lakes. Munuscong Bay is located on the western bank of the river, and is home to hundreds of hectares of wetlands. Many of the marshes in these wetlands were historically characterized by native *Schoenoplectus acutus* (Hardstem bulrush) and *Sparganium eurycarpum* (Broadfruit bur-reed) (Duffy and Batterson 1987). In recent decades, much of the emergent marsh has been converted to stands of invasive hybrid cattail. Frogbit was first detected in Munuscong Bay in 2010, and quickly spread to adjacent hybrid

cattail and *Schoenoplectus* stands (Lishawa and Alberts, MISGP 2015). The sudden appearance of frogbit in Munuscong Bay and other areas in western Michigan caused its listing as an immediate and significant threat to Michigan's aquatic ecosystems by the Michigan Department of Natural Resources.

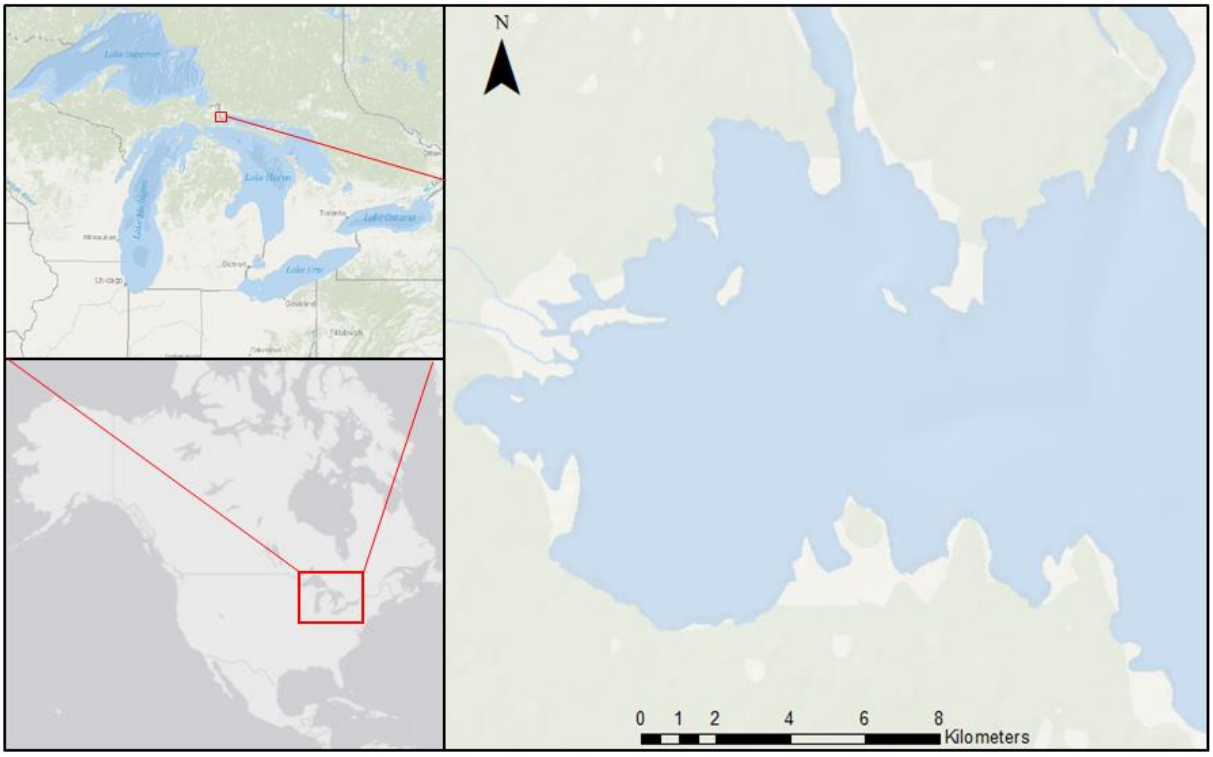

Figure 2.1 Location of Munuscong Bay in the St. Mary's River, MI

Occurrences and Processing

Occurrence records of frogbit presence in Munuscong Bay from 2014-2017 (N=572) were acquired from the Midwestern Invasive Species Network (MISIN) and collected from surveying teams from Loyola University, the Three Shores Cooperative Invasive Species Management Area, and other sources contributing to the Great Lakes Coastal Wetland Monitoring Program (GLCWMP) while surveying wetlands in Munuscong Bay. Because of the variety of sources used, detection probability, which has

been known to influence plant distribution modeling (Chen et al., 2013), was not considered in our analysis. However, because the covariates used in this model were considered at a fine grain (5m), and observation of frogbit floating mats are easily observable at this scale, error in detection probability among survey sources was assumed to be minimal. Presence-only modeling was used due to a lack of meaningful absences collected by surveyors throughout the study area. While there has been criticism of the use of presence-only records in SDMs (Yackulic et al., 2013), models predicting the potential range of invasive species have had success with limited presence records, reporting similar accuracy to models incorporating true absences (Gormley et al., 2011; West et al., 2016). However, many presence-only models suffer from sampling bias due to occurrences that are opportunistically surveyed based on ease of surveyor access (Kramer-Schadt et al., 2013). To account for this error, I created a bias layer using the "kde2d" function from the MASS package in R (Ripley 2002). This function creates a kernel density estimation of surveyor effort, which was then implemented into the model before each run. I tested two separate models, one including all covariates, and one including lidar-derived elevational data, in order to compare habitat estimates between an abiotic "Fundamental niche" topographic model, and a "Realized niche" model incorporating biotic covariates (Soberon and Peterson 2005). The sampling period (2014-2017) represented a return to long term water level averages in the Michigan-Huron basin after a 15-year low period (https://www.glerl.noaa.gov/ahps/mnth-hydro.html).

Imagery Acquisition and Processing

Lidar

Lidar data were obtained via the NOAA Digital Coast platform, hosted by the NOAA Office for Coastal Management. Data consisted of topobathy lidar collected at 10 kHz that were classified into Non-ground, Ground, and Bathymetric point, at a reported 19 cm vertical error. Data were collected by Coastal Zone Mapping and Imaging Lidar (CZMIL) over Munuscong Bay in July 2013. Although mean monthly water levels increased by roughly 70 cm from 2013-2017, St. Mary's emergent wetlands have been observed to be historically resilient in community configuration during periods of moderate water-depth fluctuations (Duffy and Batterson 1987), and examination of Landsat images did not reveal changes in their spatial extent. Density of the pulsed lidar returns was reported to be roughly 8 points/m^2. Data were buffered to reduce artifacts using Boise Center Aerospace Laboratory (BCAL) lidar tools (http://bcal.boisestate.edu/tools/lidar), a grid-based classification algorithm that uses different interpolation methods based on the desired vegetation, intensity, or topographic raster product (Montealegre et al., 2015). Spatially explicit vegetation metrics using BCAL lidar tools have previously been used in terrestrial applications characterizing sagebrush canopy (Mitchell et al., 2011), and topography from lidar have seen use in wetland plant SDMs (Sadro et al., 2007; Andrew and Ustin 2009). Buffered lidar point files were subsequently height filtered (Streutker and Glenn, 2006). Height filtered data were processed into vegetation and topographic raster layers at 5m resolution in Harris Geospatial ENVI software, and then exported to ArcMap to process for use as habitat covariates (Table 2.1). I created one abiotic and four abiotic covariates from these data.

In addition, the abiotic covariate, minimum bare-earth elevation above sea level (EleMin), was included due to previous findings of elevation and other topographic variables as strong predictors in wetland plant SDMs (Long et al., 2017; Carlson Mazur et al., 2014). Biotic covariates were vegetation cover (VegCover), the % cover of lidar point returns automatically classified as vegetation in a pixel. Vegetation height (VegHeight), the median height of vegetation returns. Vegetation height (interquartile range) (VegInt), and vegetation absolute roughness (AbsRough), the standard deviation of vegetation return heights in a pixel. These four covariates were included incorporate frogbit's observed interactions with marsh architecture into the model.

Table 2.1 List and description of each covariate used in the models. (*) Denotes inclusion into the model after pairwise removal of correlated covariates

(1) RapidEye Multispectral Imagery

(2) NOAA Digital Coast Topobathy Lidar

(3) ESA Sentinel-1 C-band SAR.

Variable	Habitat Characteristic	Type	Source
NDVI*	Plant community differentiation	Biotic	(1)
NDRE	Plant community differentiation	Biotic	(1)
EleMin*	Bare earth minimum elevation	Abiotic	(2)
VegCover*	Marsh stand architecture	Biotic	(2)
VegHeight	Marsh stand architecture	Biotic	(2)
VegINT	Marsh stand architecture	Biotic	(2)
AbsRough	Marsh stand architecture	Biotic	(2)
VVChange*	Inundation seasonality in marsh zone	Biotic	(3)
VHChange*	Phenology change in plant canopies	Biotic	(3)
JanVV	Shaded area marsh stands reducing frogbit recruitment	Biotic	(3)

Multispectral

A multispectral RapidEye image of 721 sq. km in Munuscong Bay and the St. Mary's River was captured on August 29th, 2016, and delivered as an orthorectified image at 5m resolution. RapidEye imagery contains five bands (blue (440-550nm), green (520-590nm), red (630-685nm), red-edge (630-685nm), and near-infrared (760-850nm). The red, red-edge, and near-infrared bands were used to create a Normalized Difference Vegetation Index (NDVI) and Normalized Difference Red Edge Index (NDRE) (Table

2.1), which are commonly used in ecological studies as a sign of generalized plant productivity (Pettorelli et al., 2005).

Synthetic Aperture Radar

ESA Sentinel-1 C-band SAR data were obtained from the Alaska Satellite Facility's data portal. C-band SAR imagery from the Sentinel-1 comes in two polarizations, vertical transmit and receive (VV), and cross-polarized vertical transmit horizontal receive (VH). The VV polarization has shown in previous wetland remote sensing studies an ability to measure soil moisture and inundation due to a "double bounce" effect (Bourgeau-Chavez et al., 2005). The VH polarization in contrast has typically been utilized in ecological studies as a measure of biomass (Kasischke et al., 1997). I created three covariates from metrics derived from these two polarizations: "VVChange", "VHChange, and "JanVV" (Table 2.1). An individual VV scene on January 7th, 2017 (JanVV) was included based on field observations of permanent standing litter in shallow areas of hybrid cattail stands during the winter, and the absence of frogbit in such areas during the summer months (occurrence data included in Appendex B.1). The two other SAR covariates that were included (VVChange and VHChange) measured temporal change in inundation and biomass conditions via a ratio in backscatter intensity from May-August 2016 during the growing season. SAR change detection, especially using the VV polarization, has previously been used in remote sensing studies to determine the extent of flooding (Brisco et al., 2013), and ecotype classification (Simard et al., 2000). SAR data processing used the Sentinel Application Platform (SNAP), which included applying an orbital file, SI thermal noise correction, radiometric calibration to sigma0, a 3x3 window median speckle filter, and range-doppler

terrain correction. See (Moreira et al., 2013) for processing and calibration techniques used in SNAP.

Covariate and Model Selection

A priori, I identified 10 variables I hypothesized influenced the distribution of frogbit in Munuscong Bay, ultimately using five for the model runs: NDVI, minimum elevation (EleMin), vegetation cover (VegCover), marsh inundation seasonality (VVChange), and plant canopy phenology change (VHChange) (Table 2.1). To decrease multicollinearity, I created a pairwise correlation matrix (Pearson's r) for all 10 covariates (Appendix B.2), and removed covariates until all pairwise correlations were smaller than a recommended threshold of 0.7 (Dormann et al., 2013). An exception was made in the case of the two radar coherency covariates (VVCHANGE and VHCHANGE), as they were only slightly above the threshold (r = 0.706), and each are thought to both be ecologically meaningful based on field studies of frogbit cover in emergent wetlands (Halpern 2017). All covariates were resampled to a working resolution of 5 m.

Habitat Suitability Modeling

I used the Maxent SDM algorithm (Phillips et al., 2004; Phillips and Dudík 2008) to model the habitat suitability of frogbit in Munuscong Bay. Maxent uses species presence locations with a set of environmental predictors, and compares the conditions at these presence locations with background points containing no occurrences. Maxent has been widely used in SDM literature and was an ideal modeling algorithm for this study due to its use of presence-only samples and its robustness to field validation (West et al., 2016). Maxent has shown to perform similarly to other niche modeling software (Padalia

et al., 2014; Renner and Warton 2013). The regularization parameter, which acts as a penalty to model overfitting, was set as the default of 1, with product and hinge features removed, and 10 replicates (Merow et al., 2013). Training data was set as 70% of occurrences, with testing data at 30% to generate a mean *area under* the receiver operating characteristic *curve* (AUC) value among the 10 replicates. AUC is widely used as a measure of model performance in SDM studies, representing the probability that a random occurrence point is ranked higher in the model than a random background point, with a score of 0.5 indicating a neutral model (Fielding and Bell 1997).

Model Evaluation

Use of AUC values alone to generalize model performance has received some criticism for weaknesses in measuring actual model fit and determining a threshold in binary predictions of suitability (Lobo et al., 2008). To supplement AUC, I also evaluated each model with the True Skill Statistic (TSS = sensitivity (omission error) + specificity (commission error) – 1), to generate a presence/absence threshold of suitability (Allouche et al., 2006). Individual covariate importance and response were determined using Maxent's intrinsic Jackknife function, which measures importance by running the model and testing the gain, a measurement of relative probability of presence locations to background points, using that covariate alone (Phillips et al., 2004). Both biotic "Realized" and Elevation-only "Fundamental" habitat models were projected into binary maps of habitat suitability using ArcMap using the threshold established by the model TSS to compare their predicted habitat extents.

Results

Covariate Importance

Among the five covariates used in the Biotic model, minimum elevation (EleMin) was the most important in predicting frogbit habitat suitability in Munuscong Bay, followed in descending order of importance by plant community differentiation (NDVI), vegetation cover (VegCover), marsh inundation seasonality (VVChange), and plant canopy phenology (VHChange) (Table 2.2).

Table 2.2 Percent Contribution of Each Covariate in the Biotic "Realized" Habitat Model

Covariate	Percent contribution (%)
EleMin	42.4
NDVI	35.4
VegCover	15.4
VVChange	6.6
VHChange	0.2

Model Performance

Mean AUC values across all 10 replicates were very high for both the Realized and Fundamental habitat models. Mean TSS scores were similarly high, indicating a high agreement between the training and testing sets of data across replicates.

Table 2.3 AUC and TSS Scores for Biotic and Elevation Models

	Biotic Model	Elevation-Only

AUC	0.943	0.932
TSS	0.825	0.831

Distribution Maps

The binary suitable/unsuitable habitat maps of frogbit for both models, using the TSS score (0.83) as a threshold, indicated large areas of wetland habitat suitable to frogbit expansion (Fig. 2.2). Predictably, the Elevation-only "Fundamental" model, while having a high AUC score in the context of the entirety of Munuscong Bay (Table 3.3), predicted frogbit habitat to a much greater extent than that of the Biotic "Realized" model. Both models predicted areas in the Munuscong Wildlife Management Area, historically diked to produce waterfowl habitat, as vulnerable to increased presence of frogbit (Fig. 2.2). Additionally, both models predicted suitable habitat that continues north of all known occurrences, indicating that frogbit is likely to continue to expand in Munuscong Bay wetlands beyond its known locations (Appendix B.1).

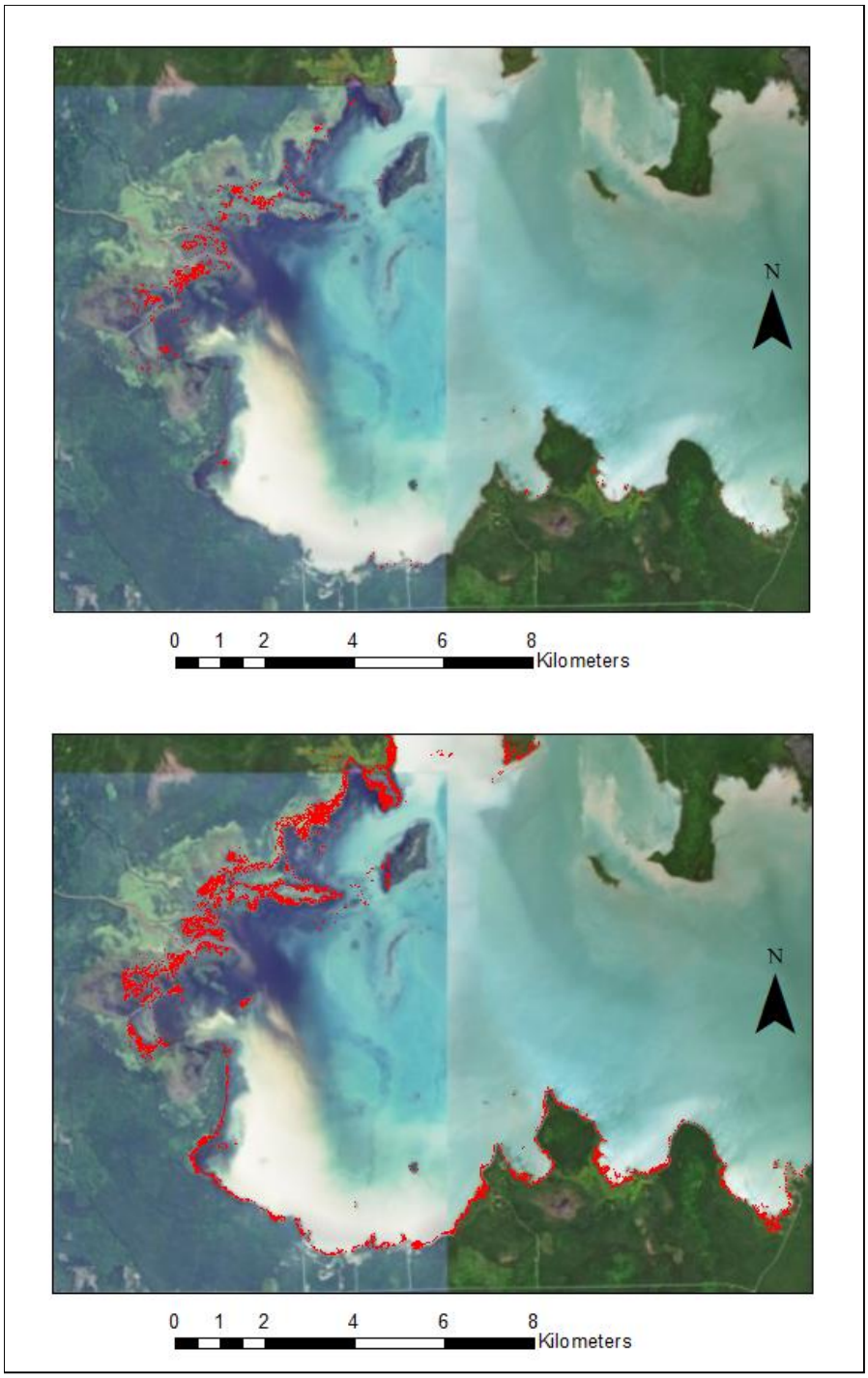

Figure 2.2 Predicted Habitat Suitability (Red) of Frogbit in Munuscong Bay (Chippewa County, MI, USA) in a Realized Habitat (Top) and Fundamental Habitat (Below) Prediction Model

Response Curve to Vegetation Cover

Vegetation cover (VegCover) was the third most important covariate overall (Table 2.2), and the second most important biotic variable before NDVI. The response curve of frogbit habitat suitability to vegetation cover indicates a tendency of frogbit to prefer emergent marsh with 20-40% cover, declining sharply below and above this range (Fig. 2.3).

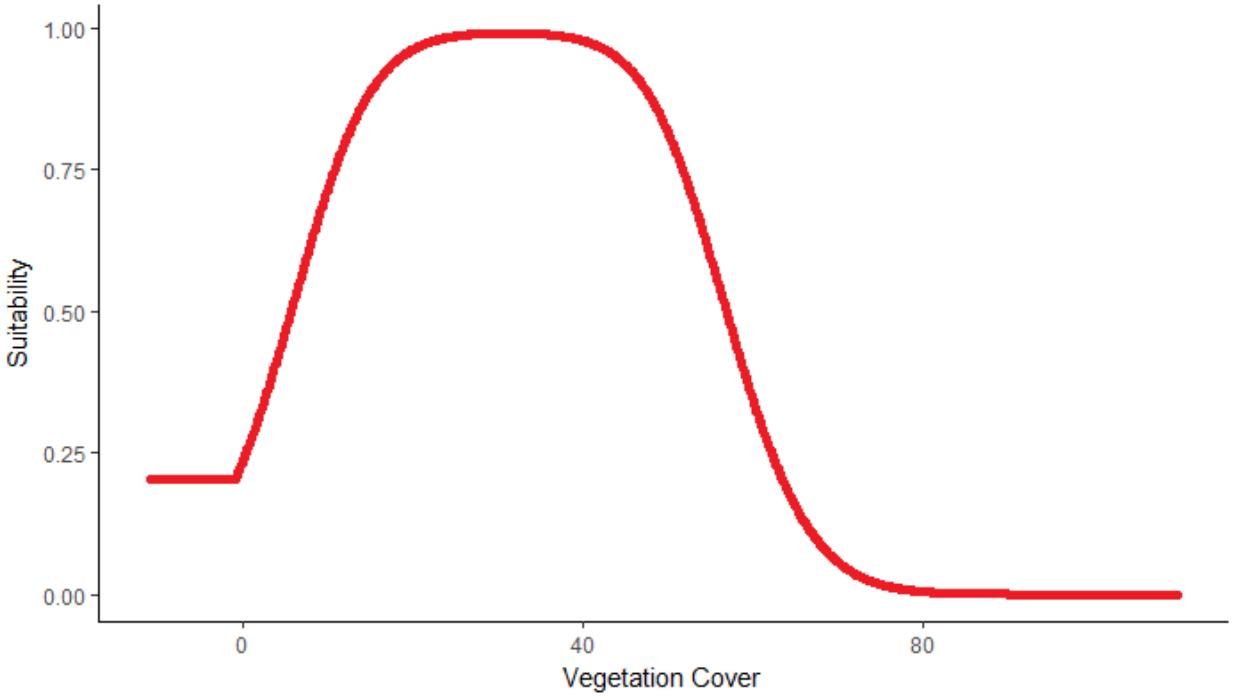

Figure 2.2 Response Curve of Frogbit Habitat Suitability to Lidar-Derived Vegetation Cover (VegCover, %)

Discussion

Lidar and Radar Contribution

The lidar-derived covariates, EleMin and VegCover, were the first and third most important covariates, respectively. Minimum elevation's strength as a covariate is in agreement with other studies that have incorporated topography in wetland SDM's (Long et al., 2017; Carlson Mazur et al., 2014). However, the relationship between minimum

elevation on the actual ecology of frogbit can be difficult to interpret. Minimum elevation predicted a narrow range of topography suitable to frogbit (roughly 175.3 meters above sea level) (Fig. 2.2). While this narrow elevation band identifies the coastal area frogbit recently established in, it could be lead to under prediction of habitat extent in upland palustrine wetlands during normal water level conditions. These results are in agreement with Andrew and Ustin (2009), that lidar-derived elevation is likely one of the few remotely sensed data sources with a vertical accuracy suitable for wetland plant SDMs. However, UAV's have since become more commonplace in ecological monitoring, and may serve as an alternative source of topographical data at a scale relevant to wetland elevation gradients.

Frogbit's habitat suitability response to vegetation cover (VegCover) (Fig. 2.3) was similar to observations made in the field of frogbit's association with hybrid cattail stands in the St. Mary's River (Lishawa, MISGP 2015). Although frogbit has been observed in many coastal wetlands that represent an emergent wetland habitat, it has also been observed as a free-floating colonial mat with no emergent plant association (Catling and Dore 1982). Additionally, field studies by Halpern et al., (2017) observed differences in turion recruitment and growth depending on frogbit's vegetation associations, highlighting the variety of growth forms frogbit populations can take. It may be that the range of vegetation cover that frogbit responded to in this model represents an ideal range, where vegetation density is sufficient enough to protect frogbit from wave energy, but sparse enough to allow for turion recruitment.

Although one radar-derived vegetation covariate, marsh inundation change (VVChange) made a contribution to the model (Table 2.2), both radar-derived vegetation

metrics performed the poorest out of the five covariates. This result is likely due to the scale of the SAR imagery (at 10 meters) compared to the other covariates (which were processed to five meters). Due to the nature of the resolution at which the data are gathered in their raw form, SAR imagery tends to be "speckled" (Bamler and Hartl 1998). Speckling may have resulted in a wide range of values for both radar-derived covariates, weakening their predictive ability in the SDM. Nonetheless, radar should be continued to be explored for spatially-explicit habitat covariates, albeit at a coarser scale than this study.

NDVI was the second-strongest covariate in the model of frogbit habitat suitability. However, caution should be exercised when generalized vegetation metrics such as NDVI are used in mapping potential habitat in SDMs, as they can instead act as correlates of current distribution rather than potential distribution (Bradley et al., 2012). For example, in my study area, large stands of invasive *Phragmites australis* that are found in southern Great Lakes coastal wetlands are absent. However, these *Phragmites* stands have become an associate of frogbit in coastal wetlands of Saginaw Bay, Michigan (CISMA manager, personal communication). If there is a possibility of frogbit invading novel marsh communities in the geographic extent of a modeling area, NDVI may under-predict these communities as suitable habitat. This consideration would have needed to be taken into account if this study was conducted in an area with extensive stands of *Phragmites*.

Distributional Maps and Limitations

While AUC and TSS values were similar for both the Biotic and Elevation-only model (Table 2.3), the Elevation-only model likely over-predicted frogbit habitat in

Munuscong Bay. While wetlands are naturally found at elevation sinks, or transitionary areas, Great Lakes coastal wetlands are also structured by wave energy and sedimentation (Albert 2003). Many of the areas predicted to be suitable for habitat for frogbit by the "Fundamental" elevation-only habitat model are sedge meadows that have limited inundation during the year. Sedges may outcompete frogbit for the light needed for turion recruitment, which would make these areas unsuitable for frogbit expansion. However, because the geographic extent of the modeling effort was the entirety of the bay, including aquatic and terrestrial habitats, AUC's remained high. This has been noted as a limitation of AUC, as a restricted habitat range, such as a band of coastal wetlands, will produce naturally high values (McPherson and Jetz 2007).

Due to a reliance on multi-source occurrence data that often suffers from spatial autocorrelation and sampling intensity issues, a Maxent bias layer was included to downsample areas with clustered sampling. However, this is by no means a perfect solution, and a model with more informed absences would be preferable. A balance must be met between accurate predictions and the strength of inference (Peters 1991). With a new invasion, it can be difficult to assume good absence data when current frogbit spatial extent may be constrained by dispersal variables that may operate on a year-to year basis in terms of sensitivity to inference (Vaclavik and Meentemeyer 2012).

Management Recommendations

Recent and ongoing experiments are exploring new ways to control large populations of established frogbit in Munuscong Bay, but management of small populations remains the optimal and most likely scenario to be effective. Managers seeking to control frogbit spread during early stages should determine if their population

is free floating, or associated with emergent wetlands, as each may have different growth habits and patterns (Halpern et al., 2017). Free-floating populations may be immediately detected when populations are large enough to be captured by the pixel size of the imagery used (Proctor et al., 2012). However, if frogbit is associated with emergent wetlands, and still inconspicuous to aerial imagery, I recommend the modeling procedures presented here to prioritize areas most suitable to frogbit expansion. Covariates which include biotic interactions (Such as marsh inundation and vegetation cover estimates from radar and lidar) will incorporate their ecological potential in a landscape, rather than a crude geographic estimate.

Further investigation should focus on frogbit abundance and cover, and interrelatedness with shade and physical habitat structure. (Zhu et al., 2014) found that at certain shading thresholds, frogbit abundance decreases or is nonpresent. Fine tuning "occurrence" with "abundance" might explain more about the ecology of the species and help further delineate areas where the shading mechanisms of dense frogbit mats may have the most effect. Disperal covariates, such as distance to boat launches, may also warrant consideration for inclusion into models that predict frogbit habitat suitability and range expansion at scales larger than Munuscong Bay.

Conclusions

This modeling effort examined two novel data sources not commonly used in niche modeling at a landscape scale. By including lidar and radar-derived vegetation metrics, I was able to predict the future expansion of an inconspicuous invasive wetland plant. While lidar-derived elevation was an important covariate in the model, and in wetland SDMs in general, it appears to over predict the amount of wetland area at risk to

frogbit invasion. NDVI, vegetation cover, and marsh inundation shifts over the growing season were ecologically meaningful covariates that limited the predictions made by elevation to the species-specific habitat interactions of frogbit in coastal wetlands. However, because coastal wetland species may only be found in a narrow area of a landscape, geographic extent of the modeling effort must be considered when selecting meaningful covariates and inferring model performance results.

Remote sensing continues to advance as a field, providing cost-effective products for ecological modeling efforts. In terms of ecological studies, the challenge becomes interpretation of those patterns by a user that has knowledge of general or local ecological conditions. Bridging these gaps and incorporating new technology (such as variables derived from UAV imagery/point clouds) into a modeling framework will allow SDMs and other predictive niche models to allow for more inference by ecologists than the broad climate-based variables that have been traditionally used in most SDM studies. Such an effort may contribute to both a better understanding of an ongoing invasion, and are likely to contribute to effective management of an invasion.

REFERENCES

Adam, E., Mutanga, O., Odindi, J., Abdel-Rahman, E.M., 2014. Land-use/cover classification in a heterogeneous coastal landscape using RapidEye imagery: evaluating the performance of random forest and support vector machines classifiers. Int. J. Remote Sens. 35, 3440–3458. doi:10.1080/01431161.2014.903435

Adam, E., Mutanga, O., Rugege, D., 2010. Multispectral and hyperspectral remote sensing for identification and mapping of wetland vegetation: A review. Wetl. Ecol. Manag. 18, 281–296. doi:10.1007/s11273-009-9169-z

Albert, D., 2003. Between land and lake: Michigan's Great Lakes coastal wetlands. Extension Bulletin E-2902.

Allouche, O., Tsoar, A., Kadmon, R., 2006. Assessing the accuracy of species distribution models: prevalence, Kappa and the True Skill Statistic (TSS), Journal of Applied Ecology. doi:10.1111/j.1365-2664.2006.01214.x

Andrew, M.E., Ustin, S.L., 2009. Habitat suitability modelling of an invasive plant with advanced remote sensing data. Divers. Distrib. 15, 627–640. doi:10.1111/j.1472-4642.2009.00568.x

Ayers, D.R., Smith, D.L., Zaremba, K., Klohr, S., Strong, D.R., 2004. Spread of Exotic Cordgrasses and Hybrids (<Emphasis Type="Italic">Spartina</Emphasis> sp.) in the Tidal Marshes of San Francisco Bay, California, USA - art%3A10.1023%2FB%3ABINV.0000022140.07404.b7.pdf. Biol. Invasions 6, 221–231. doi:10.1023/B:BINV.0000022140.07404.b7

Baghdadi, N., Bernier, M., Gauthier, R., Neeson, I., 2001. Evaluation of C-band SAR data for wetlands mapping. Int. J. Remote Sens. 22, 71–88. doi:10.1080/014311601750038857

Bamler, R., Hartl, P., 1998. Synthetic aperture radar interferometry. Inverse Prob. 14, R1.

Beaumont, L.J., Hughes, L., Poulsen, M., 2005. Predicting species distributions : use of climatic parameters in BIOCLIM and its impact on predictions of species ' current and future distributions 186, 250–269. doi:10.1016/j.ecolmodel.2005.01.030

Booth, T.H., Nix, H.A., Busby, J.R., Hutchinson, M.F., 2014. Bioclim: The first species distribution modelling package, its early applications and relevance to most current MaxEnt studies. Divers. Distrib. 20, 1–9. doi:10.1111/ddi.12144

Bourgeau-Chavez, L., Endres, S., Battaglia, M., Miller, M. E., Banda, E., Laubach, Z., ... & Marcaccio, J., 2015. Development of a bi-national Great Lakes coastal wetland and land use map using three-season PALSAR and Landsat imagery. Remote Sens. 7, 8655–8682.

Bourgeau-Chavez, L., Riordan, K., Miller, N., Nowels, M., 2009. Improving wetland characterization with multi- sensor , multi-temporal SAR and optical / infrared data fusion 679–708.

Bourgeau-Chavez, L.L., Kasischke, E.S., Brunzell, S.M., Mudd, J.P., Smith, K.B., Frick, A.L., 2001. Analysis of space-borne SAR data for wetland mapping in Virginia riparian ecosystems. Int. J. Remote Sens. 22, 3665–3687. doi:10.1080/01431160010029174

Bourgeau-Chavez, L.L., Smith, K.B., Brunzell, S.M., Kasischke, E.S., Romanowicz, E. a., Richardson, C.J., 2005. Remote monitoring of regional inundation patterns and hydroperiod in the Greater Everglades using Synthetic Aperture Radar. Wetlands 25, 176–191. doi:10.1672/0277-5212(2005)025[0176:RMORIP]2.0.CO;2

Bradley, B.A., Olsson, A.D., Wang, O., Dickson, B.G., Pelech, L., Sesnie, S.E., Zachmann, L.J., 2012. Species detection vs. habitat suitability: Are we biasing habitat suitability models with remotely sensed data? Ecol. Modell. 244, 57–64. doi:10.1016/j.ecolmodel.2012.06.019

Breiman, L., 2001. Random forests. Mach. Learn. 45, 5–32. doi:10.1023/A:1010933404324

Breiman, L., 1999. Random Forests. Mach. Learn. 45, 1–35. doi:10.1023/A:1010933404324

Brisco, B., Schmitt, A., Murnaghan, K., Kaya, S., Roth, A., 2013. SAR polarimetric change detection for flooded vegetation. Int. J. Digit. Earth 6, 103–114. doi:10.1080/17538947.2011.608813

Brock, J.C., Purkis, S.J., 2009. The Emerging Role of Lidar Remote Sensing in Coastal Research and Resource Management. J. Coast. Res. 10053, 1–5. doi:10.2112/SI53-001.1

Buermann, W., Saatchi, S., Smith, T.B., Brian, R., Graham, C.H., Chaves, J.A., Mila, B., 2008. Predicting species distributions across the Amazonian and Andean regions using remote sensing data 1160–1176. doi:10.1111/j.1365-2699.2007.01858.x

Bullock, A., Acreman, M., Bullock, A., Bullock, A., Acreman, M., 2003. The role of wetlands in the hydrological cycle To cite this version : HAL Id : hal-00304786 The role of wetlands in the hydrological cycle 7, 358–389.

Bunbury-Blanchette, A.L., Freeland, J.R., Dorken, M.E., 2015. Hybrid Typha × glauca outperforms native T. latifolia under contrasting water depths in a common garden. Basic Appl. Ecol. 16. doi:10.1016/j.baae.2015.04.006

Carlson Mazur, M.L., Kowalski, K.P., Galbraith, D., 2014. Assessment of suitable habitat for Phragmites australis (common reed) in the Great Lakes coastal zone. Aquat. Invasions 9, 1–19. doi:10.3391/ai.2014.9.1.01

Carreiras, J.M.B., Melo, J.B., Vasconcelos, M.J., 2013. Estimating the above-ground biomass in miombo savanna woodlands (Mozambique, East Africa) using L-band synthetic aperture radar data. Remote Sens. 5, 1524–1548. doi:10.3390/rs5041524

Catling, P. M., & Dore, W.G., 1982. Status and identification of Hydrocharis morsus-ranae and Limnobium spongia (Hydrocharitaceae) in northeastern North America. Rhodora 523–545.

Catling, P.M., Mitrow, G., Haber, E., Posluszny, U., Charlton, W.A., 2003. The biology of Canadian weeds . 124 . Hydrocharis morsus-ranae L . 7, 5–7.

Chen, G., Kéry, M., Plattner, M., Ma, K., Gardner, B., 2013. Imperfect detection is the rule rather than the exception in plant distribution studies. J. Ecol. 101, 183–191. doi:10.1111/1365-2745.12021

Ciotir, C., Kirk, H., Row, J.R., Freeland, J.R., 2013. Intercontinental dispersal of Typha angustifolia and T. latifolia between Europe and North America has implications for Typha invasions. Biol. Invasions 15. doi:10.1007/s10530-012-0377-8

Clavero, M., García-Berthou, E., 2005. Invasive species are a leading cause of animal extinctions 20, 5451. doi:10.1016/j.tree.2005.01.003

Cohen Warren, B., Parker Geoffrey, G., Harding David, J., Lefsky, M., 2002. Lidar remote sensing for ecosystem studies. Bioscience 52, 19–30. doi:10.1641/0006-3568(2002)052[0019:LRSFES]2.0.CO;2

Corcoran, J.M., Knight, J.F., Gallant, A.L., 2013. Influence of multi-source and multi-temporal remotely sensed and ancillary data on the accuracy of random forest classification of wetlands in northern Minnesota. Remote Sens. 5, 3212–3238. doi:10.3390/rs5073212

Crall, A.W., Jarnevich, C.S., Panke, B., Young, N., Renz, M., Morisette, J., 2013. Using habitat suitability models to target invasive plant species surveys. Ecol. Appl. 23, 60–72. doi:10.1890/12-0465.1

Crooks, J. A., Soulé, M. E., & Sandlund, O.T., 1999. Lag times in population explosions of invasive species: causes and implications. Invasive species Biodivers. Manag. 103–125.

Crookston, N.L., Finley, a O., 2008. yaImpute: An R package for κNN imputation. J. Stat. Softw. 23, 1–16. doi:doi:

Cutler, D.R., Edwards, T.C., Beard, K.H., Cutler, A., Hess, T., Gibson, J., Lawler, J.J., Cutler, D.R., Edwards, T.C., Beard, K.H., Cutler, A., Hess, K.T., Gibson, J., Lawler, J.J., 2007. Random Forests for Classification in Ecology Published by : Wiley on behalf of the Ecological Society of America Stable URL : http://www.jstor.org/stable/27651436 RANDOM FORESTS FOR CLASSIFICATION IN ECOLOGY. Ecology 88, 2783–2792.

Cvetkovic, M., Chow-Fraser, P., 2011. Use of ecological indicators to assess the quality of Great Lakes coastal wetlands. Ecol. Indic. 11, 1609–1622. doi:10.1016/j.ecolind.2011.04.005

Dahl, T.E., 1990. Wetlands losses in the United States, 1780's to 1980's. Report to the Congress (No. PB-91-169284/XAB). National Wetlands Inventory, St. Petersburg, FL (USA).

Delegido, J., Verrelst, J., Alonso, L., Moreno, J., 2011. Evaluation of sentinel-2 red-edge bands for empirical estimation of green LAI and chlorophyll content. Sensors 11, 7063–7081. doi:10.3390/s110707063

Dormann, C.F., Elith, J., Bacher, S., Buchmann, C., Carl, G., Carré, G., Marquéz, J.R.G., Gruber, B., Lafourcade, B., Leitão, P.J., Münkemüller, T., Mcclean, C., Osborne, P.E., Reineking, B., Schröder, B., Skidmore, A.K., Zurell, D., Lautenbach, S., 2013. Collinearity: A review of methods to deal with it and a simulation study evaluating their performance. Ecography (Cop.). 36, 027–046. doi:10.1111/j.1600-0587.2012.07348.x

Duffy, W.G., Batterson, T.R., 1987. The St. Mary's River, Michigan: An ecological profile. U. S. Fish and Wildlife Service, Washington, DC, USA. Biol. Rep. 87(7.10).

Elith, J., Leathwick, J.R., 2009. Species Distribution Models: Ecological Explanation and Prediction Across Space and Time. Annu. Rev. Ecol. Evol. Syst. 40, 677–697. doi:10.1146/annurev.ecolsys.110308.120159

Ellstrand, N.C., Schierenbeck, K.A., 2000. Hybridization as a stimulus for the evolution of invasiveness in plants ? 97, 7043–7050.

Eppers, M.E., Rudstam, L.G., Heide, V. Der, Colleges, W.S., 2008. Predicting Invasion of European Frogbit in the Finger Lakes of New York 186–189.

Ficetola, G.F., Bonardi, A., Mücher, C.A., Gilissen, N.L.M., Padoa-Schioppa, E., 2014. How many predictors in species distribution models at the landscape scale? Land use versus LiDAR-derived canopy height. Int. J. Geogr. Inf. Sci. 28, 1723–1739. doi:10.1080/13658816.2014.891222

Fielding, A.H., Bell, J.F., 1997. A review of methods for the assessment of prediction errors in conservation presence / absence models. Environ. Conserv. 24, 38–49. doi:10.1017/S0376892997000088

Filella, I., Penuelas, J., 1994. The red edge position and shape as indicators of plant chlorophyll content, biomass and hydric status. Int. J. Remote Sens. 15, 1459–1470. doi:10.1080/01431169408954177

Franklin, J., Davis, F.W., Ikegami, M., Syphard, A.D., Flint, L.E., Flint, A.L., Hannah, L., 2013. Modeling plant species distributions under future climates: How fine scale do climate projections need to be? Glob. Chang. Biol. 19, 473–483. doi:10.1111/gcb.12051

Frieswyk, C.B., Johnston, C.A., Zedler, J.B., 2007. Identifying and Characterizing Dominant Plants as an Indicator of Community Condition. J. Great Lakes Res. 33, 125–135. doi:10.3394/0380-1330(2007)33[125:IACDPA]2.0.CO;2

Gallant, A.L., 2015. The challenges of remote monitoring of wetlands. Remote Sens. 7, 10938–10950. doi:10.3390/rs70810938

Gibbs, J.P., 2016. Society for Conservation Biology Wetland Loss and Biodiversity Conservation Published by : Wiley for Society for Conservation Biology Stable URL : http://www.jstor.org/stable/2641930 Linked references are available on JSTOR for this article : You may need 14, 314–317.

Gormley, A.M., Forsyth, D.M., Griffioen, P., Lindeman, M., Ramsey, D.S.L., Scroggie, M.P., Woodford, L., 2011. Using presence-only and presence-absence data to estimate the current and potential distributions of established invasive species. J. Appl. Ecol. 48, 25–34. doi:10.1111/j.1365-2664.2010.01911.x

Guarnieri, A., Vettore, A., Pirotti, F., Menenti, M., Marani, M., 2009. Retrieval of small-relief marsh morphology from Terrestrial Laser Scanner, optimal spatial filtering, and laser return intensity. Geomorphology 113, 12–20. doi:10.1016/j.geomorph.2009.06.005

Guisan, A., Thuiller, W., 2005. Predicting species distribution: Offering more than simple habitat models. Ecol. Lett. 8, 993–1009. doi:10.1111/j.1461-0248.2005.00792.x

Halpern, A.D., 2017. *Hydrocharis morsus-ranae* in the upper St. Lawrence River in New York: Its success within heterogenous wetland habitat and potential management approaches (Doctoral dissertation). State University of New York.

He, K.S., Rocchini, D., Neteler, M., Nagendra, H., 2011. Benefits of hyperspectral remote sensing for tracking plant invasions. Divers. Distrib. 17, 381–392. doi:10.1111/j.1472-4642.2011.00761.x

Hejda, M., Py, P., 2009. Impact of invasive plants on the species richness , diversity and composition of invaded communities 393–403. doi:10.1111/j.1365-2745.2009.01480.x

Hess, L.L., Melack, J.M., Novo, E.M.L.M., Barbosa, C.C.F., Gastil, M., 2003. Dual-season mapping of wetland inundation and vegetation for the central Amazon basin. Remote Sens. Environ. 87, 404–428. doi:10.1016/j.rse.2003.04.001

Hestir, E. L., Khanna, S., Andrew, M. E., Santos, M. J., Viers, J. H., Greenberg, J. A., ... & Ustin, S.L., 2008. Identification of invasive vegetation using hyperspectral remote sensing in the California Delta ecosystem. Remote Sens. Environ. 112, 4034–4047.

Holdredge, C., Bertness, M.D., 2011. Litter legacy increases the competitive advantage of invasive Phragmites australis in New England wetlands 423–433. doi:10.1007/s10530-010-9836-2

Hong, S.H., Kim, H.O., Wdowinski, S., Feliciano, E., 2015. Evaluation of polarimetric SAR decomposition for classifying wetland vegetation types. Remote Sens. 7, 8563–8585. doi:10.3390/rs70708563

Houlahan, J.E., Findlay, C.S., 2004. Effect of Invasive Plant Species on Temperate Wetland Plant Diversity 18, 1132–1138.

Jensen, A.M., Hardy, T., McKee, M., Chen, Y.Q., 2011. Using a multispectral autonomous unmanned aerial remote sensing platform (AggieAir) for riparian and wetlands applications. Int. Geosci. Remote Sens. Symp. 3413–3416. doi:10.1109/IGARSS.2011.6049953

Jiménez-Valverde, A., Peterson, A.T., Soberón, J., Overton, J.M., Aragón, P., Lobo, J.M., 2011. Use of niche models in invasive species risk assessments. Biol. Invasions 13, 2785–2797. doi:10.1007/s10530-011-9963-4

Johnston, C.A., 1991. Sediment and nutrient retention by freshwater wetlands: Effects on surface water quality. Crit. Rev. Environ. Control 21, 491–565. doi:10.1080/10643389109388425

Jones, T.G., Coops, N.C., Sharma, T., 2010. Assessing the utility of airborne hyperspectral and LiDAR data for species distribution mapping in the coastal Pacific Northwest, Canada. Remote Sens. Environ. 114, 2841–2852. doi:10.1016/j.rse.2010.07.002

Joshi, C., De Leeuw, J., Van Andel, J., Skidmore, A.K., Lekhak, H.D., Van Duren, I.C., Norbu, N., 2006. Indirect remote sensing of a cryptic forest understorey invasive species. For. Ecol. Manage. 225, 245–256. doi:10.1016/j.foreco.2006.01.013

Jude, D. J., & Pappas, J., 1992. Fish utilization of Great Lakes coastal wetlands. J. Great Lakes Res. 18, 651–672.

Junk, W.J., Brown, M., Campbell, I.C., Finlayson, M., Gopal, B., Ramberg, L., Warner, B.G., 2006. The comparative biodiversity of seven globally important wetlands: A synthesis. Aquat. Sci. 68, 400–414. doi:10.1007/s00027-006-0856-z

Kasischke, E.S., Melack, J.M., Craig Dobson, M., 1997. The use of imaging radars for ecological applications—A review. Remote Sens. Environ. 59, 141–156. doi:10.1016/S0034-4257(96)00148-4

Keller, R.P., Frang, K., Lodge, D.M., 2008. Preventing the spread of invasive species: Economic benefits of intervention guided by ecological predictions. Conserv. Biol. 22, 80–88. doi:10.1111/j.1523-1739.2007.00811.x

Kerr, J.T., Ostrovsky, M., 2003. From space to species: Ecological applications for remote sensing. Trends Ecol. Evol. 18, 299–305. doi:10.1016/S0169-5347(03)00071-5

Kettenring, K.M., Adams, C.R., 2011. Lessons learned from invasive plant control experiments : a systematic review and meta-analysis 970–979. doi:10.1111/j.1365-2664.2011.01979.x

Knipling, E., 1970. Physical and Physiological Basis for the Reflectance of Visible and Near Infrared Radiation from Vegetation. Remote Sens. Environ. 1, 155–159.

Koch, B., 2010. Status and future of laser scanning, synthetic aperture radar and hyper-spectral remote sensing data for forest biomass assessment. ISPRS J. Photogramm. Remote Sens. 65, 581-590.

Kramer-Schadt, S., Niedballa, J., Pilgrim, J.D., Schröder, B., Lindenborn, J., Reinfelder, V., Stillfried, M., Heckmann, I., Scharf, A.K., Augeri, D.M., Cheyne, S.M., Hearn, A.J., Ross, J., Macdonald, D.W., Mathai, J., Eaton, J., Marshall, A.J., Semiadi, G., Rustam, R., Bernard, H., Alfred, R., Samejima, H., Duckworth, J.W., Breitenmoser-Wuersten, C., Belant, J.L., Hofer, H., Wilting, A., 2013. The importance of correcting for sampling bias in MaxEnt species distribution models. Divers. Distrib. 19, 1366–1379. doi:10.1111/ddi.12096

Lang, M.W., Kasischke, E.S., Prince, S.D., Pittman, K.W., 2008. Assessment of C-band synthetic aperture radar data for mapping and monitoring Coastal Plain forested wetlands in the Mid-Atlantic Region, U.S.A. Remote Sens. Environ. 112, 4120–4130. doi:10.1016/j.rse.2007.08.026

Lass, L.W., Prather, T.S., Glenn, N.F., Weber, K.T., Mundt, J.T., Pettingill, J., 2005. A review of remote sensing of invasive weeds and example of the early detection of spotted knapweed (*Centaurea maculosa*) and babysbreath (*Gyp-sophila paniculata*) with a hyperspectral sensor. Weed Science, 53, 242–251.Legendre P. 1993. Spatial autocorrelation: trouble or new paradigm? Ecology 74:1659–73

Leung, B., Lodge, D.M., Finnoff, D., Shogren, J.F., Lewis, M.A., Lamberti, G., 2002. An ounce of prevention or a pound of cure: bioeconomic risk analysis of invasive species. Proc. R. Soc. B Biol. Sci. 269, 2407–2413. doi:10.1098/rspb.2002.2179

Liao, C., Peng, R., Luo, Y., Zhou, X., Wu, X., Fang, C., Chen, J., Li, B., Li, B., 2006. Altered ecosystem carbon and nitrogen cycles by plant invasion : a meta-analysis 706–714.

Liaw, a, Wiener, M., 2002. Classification and Regression by randomForest. R news 2, 18–22. doi:10.1177/154405910408300516

Liaw, A., Wiener, M., 2014. RandomForest. R news XXXIX, 54.1-54.10. doi:10.5244/C.22.54

Lishawa, S.C., Carson, B.D., Brandt, J.S., Tallant, J.M., Reo, N.J., Albert, D.A., Monks, A.M., Lautenbach, J.M., Clark, E., 2017. Mechanical Harvesting Effectively Controls Young Typha spp. Invasion and Unmanned Aerial Vehicle Data Enhances Post-treatment Monitoring. Front. Plant Sci. 8, 1–14. doi:10.3389/fpls.2017.00619

Lishawa, S.C., Lawrence, B.A., Albert, D.A., Tuchman, N.C., 2015. Biomass harvest of invasive Typha promotes plant diversity in a Great Lakes coastal wetland. Restor. Ecol. 23, 228–237.

Lobo, J.M., Jiménez-valverde, A., Real, R., 2008. AUC: A misleading measure of the performance of predictive distribution models. Glob. Ecol. Biogeogr. 17, 145–151. doi:10.1111/j.1466-8238.2007.00358.x

Lodge, D.M., Simonin, P.W., Burgiel, S.W., Keller, R.P., Bossenbroek, J.M., Jerde, C.L., Kramer, A.M., Rutherford, E.S., Barnes, M.A., Wittmann, M.E., Chadderton, W.L., Apriesnig, J.L., Beletsky, D., Cooke, R.M., Drake, J.M., Egan, S.P., Finnoff, D.C., Gantz, C.A., Grey, E.K., Hoff, M.H., Howeth, J.G., Jensen, R.A., Larson, E.R., Mandrak, N.E., Mason, D.M., Martinez, F.A., Newcomb, T.J., Rothlisberger, J.D., Tucker, A.J., Warziniack, T.W., Zhang, H., 2016. Risk Analysis and Bioeconomics of Invasive Species to Inform Policy and Management. Annu. Rev. Environ. Resour. 41, 453–488. doi:10.1146/annurev-environ-110615-085532

Long, A.L., Kettenring, K.M., Hawkins, C.P., Neale, C.M.U., 2017. Distribution and Drivers of a Widespread, Invasive Wetland Grass, Phragmites australis, in

Wetlands of the Great Salt Lake, Utah, USA. Wetlands 37, 45–57. doi:10.1007/s13157-016-0838-4

Lussem, U., Hütt, C., Waldhoff, G., 2016. Combined analysis of Sentinel-1 and RapidEye data for improved crop type classification: An early season approach for rapeseed and cereals. Int. Arch. Photogramm. Remote Sens. Spat. Inf. Sci. - ISPRS Arch. 41, 959–963. doi:10.5194/isprsarchives-XLI-B8-959-2016

Mack RN, Simberloff D, Lonsdale WM, Evans H, Clout M, Bazzaz FA. 2000. Biotic invasions: Causes, epidemiology, global consequences, and control. Ecological Applications 10: 689–710.

Martin, L.J., Blossey, B., 2013. The Runaway Weed: Costs and Failures of Phragmites australis Management in the USA. Estuaries and Coasts 36, 626–632. doi:10.1007/s12237-013-9593-4

Martinez, J., Le Toan, T., 2007. Mapping of flood dynamics and vegetation spatial distribution in the Amazon floodplain using multitemporal SAR data. Remote Sensing of Environment. doi:10.1016/j.rse.2006.11.012

McPherson, J.M., Jetz, W., 2007. Effect of species' ecology on the accuracy of distribution models. Ecography 30, 135-151.

Mehta, S. V., Haight, R. G., Homans, F. R., Polasky, S., & Venette, R.C., 2007. Optimal detection and control strategies for invasive species management. Ecol. Econ. 61, 237–245.

Merow, C., Smith, M.J., Silander, J.A., 2013. A practical guide to MaxEnt for modeling species’ distributions: What it does, and why inputs and settings matter. Ecography (Cop.). 36, 1058–1069. doi:10.1111/j.1600-0587.2013.07872.x

Mitchell, J.J., Glenn, N.F., Sankey, T.T., Derryberry, D.R., Anderson, M.O., Hruska, R.C., 2011. Small-footprint Lidar Estimations of Sagebrush Canopy Characteristics. Photogramm. Eng. Remote Sens. 77, 521–530. doi:10.14358/PERS.77.5.521

Mitchell, M.E., Lishawa, S.C., Geddes, P., Larkin, D.J., Treering, D., Tuchman, N.C., 2011. Time-Dependent Impacts of Cattail Invasion in a Great Lakes Coastal Wetland Complex. doi:10.1007/s13157-011-0225-0

Molnar, J.L., Gamboa, R.L., Revenga, C., Spalding, M.D., 2008. Assessing the global threat of invasive species to marine biodiversity. Front. Ecol. Environ. 6, 485–492. doi:10.1890/070064

Montealegre, A.L., Lamelas, M.T., De La Riva, J., 2015. A Comparison of Open - Source LiDAR Filtering Algorithms in a Mediterranean Forest Environment. IEEE J. Sel. Top. Appl. Earth Obs. Remote Sens. 8, 4072–4085. doi:10.1109/JSTARS.2015.2436974

Moreira, A., Prats, P., Younis, M., Krieger, G., Hajnsek, I., Papathanassiou, K., 2013. A Tutorial on Synthetic Aperture Radar. IEEE Geosci. Remote Sens. Mag. 1–43. doi:10.1109/MGRS.2013.2248301

Nitze, I., Schulthess, U., Asche, H., 2012. Comparison of machine learning algorithms random forest, artificial neuronal network and support vector machine to maximum likelihood for supervised crop type classification. Proc. 4th Conf. Geogr. Object-Based Image Anal. – GEOBIA 2012 35–40.

Olden, J.D., Poff, N.L., Douglas, M.R., Douglas, M.E. & Fausch, K.D. (2004) Ecological and evolutionary consequences of biotic homogenization. Trends in Ecology and Evolution, 19, 18–24.

Olson, A., Paul, J., Freeland, J.R., 2009. Habitat preferences of cattail species and hybrids (Typha spp.) in eastern Canada. Aquat. Bot. 91, 67–70. doi:10.1016/j.aquabot.2009.02.003

Ozesmi, S.L., Bauer, M.E., 2002. Satellite remote sensing of wetlands. Wetl. Ecol. Manag. 10, 381–402. doi:10.1023/A:1020908432489

Padalia, H., Srivastava, V., Kushwaha, S.P.S., 2014. Modeling potential invasion range of alien invasive species, Hyptis suaveolens (L.) Poit. in India: Comparison of MaxEnt and GARP. Ecol. Inform. 22, 36–43. doi:10.1016/j.ecoinf.2014.04.002

Pearson, R.G., Dawson, T.P., 2003. Predicting the impacts of climate change on the distribution of species: Are bioclimate envelope models useful? Glob. Ecol. Biogeogr. 12, 361–371. doi:10.1046/j.1466-822X.2003.00042.x

Peters, R.H., 1991. A Critique for Ecology. Cambridge University Press, Cambridge, UK.

Soberón, J., Peterson, A.T., 2005. Interpretation of models of fundamental ecological niches and species' distributional areas. Biodiv. Inf. Biodiversity Informatics 2.0 (2005): n. pag. http://dx.doi.org/10.17161/bi.v2i0.4

Pettorelli, N., Vik, J.O., Mysterud, A., Gaillard, J.M., Tucker, C.J., Stenseth, N.C., 2005. Using the satellite-derived NDVI to assess ecological responses to environmental change. Trends Ecol. Evol. 20, 503–510. doi:10.1016/j.tree.2005.05.011

Phillips, S.J., Dudík, M., 2008. Modeling of species distribution with Maxent: new extensions and a comprehensive evalutation. Ecograpy 31, 161–175. doi:10.1111/j.2007.0906-7590.05203.x

Phillips, S.J., Dudík, M., Schapire, R.E., 2004. A maximum entropy approach to species distribution modeling. 21st Int. Conf. Mach. Learn. Banff, Canada 655–662. doi:10.1145/1015330.1015412

Pimentel, D., Zuniga, R., Morrison, D., 2005. Update on the environmental and economic costs associated with alien-invasive species in the United States 52, 273–288. doi:10.1016/j.ecolecon.2004.10.002

Price, A.L., Fant, J.B., Larkin, D.J., 2014. Ecology of Native vs . Introduced Phragmites australis (Common Reed) in Chicago-Area Wetlands 369–377. doi:10.1007/s13157-013-0504-z

Prince, H. H., Padding, P. I., & Knapton, R.W., 1992. Waterfowl use of the Laurentian Great Lakes. J. Great Lakes Res. 18, 673–699.

Proctor, C., Robinson, V., He, Y., 2012. Multispectral detection of European frog-bit in the South Nation River using Quickbird imagery. Can. J. Remote Sens. 38, 476–486. doi:10.5589/m12-040

Ramoelo, A., Skidmore, A.K., Cho, M.A., Schlerf, M., Mathieu, R., Heitkönig, I.M.A., 2012. Regional estimation of savanna grass nitrogen using the red-edge band of the spaceborne rapideye sensor. Int. J. Appl. Earth Obs. Geoinf. 19, 151–162. doi:10.1016/j.jag.2012.05.009

Ramsey, E.W., Laine, S.C., 1997. Comparison of Landsat Thematic Mapper and high resolution photography to identify change in complex coastal wetlands. J. Coast. Res. 13, 281–292.

Rejmánek, M., Pitcairn, M.J., 2002. When is eradication of exotic pest plants a realistic goal? Turn. tide Erad. invasive species 249–253.

Renner, I.W., Warton, D.I., 2013. Equivalence of MAXENT and Poisson Point Process Models for Species Distribution Modeling in Ecology. Biometrics 69, 274–281. doi:10.1111/j.1541-0420.2012.01824.x

Riffell, S. K., Keas, B. E., & Burton, T.M., 2001. Area and habitat relationships of birds in Great Lakes coastal wet meadows. Wetlands 21, 492–507.

Ripley, W.N.V. and B.D., 2002. Package ‘ MASS .’ Mod. Appl. Stat. with S.

Rocchini, D., Hernández-Stefanoni, J.L., He, K.S., 2015. Advancing species diversity estimate by remotely sensed proxies: A conceptual review. Ecol. Inform. 25, 22–28. doi:10.1016/j.ecoinf.2014.10.006

Rodriguez-Galiano, V.F., Ghimire, B., Rogan, J., Chica-Olmo, M., Rigol-Sanchez, J.P., 2012. An assessment of the effectiveness of a random forest classifier for land-cover classification. ISPRS J. Photogramm. Remote Sens. 67, 93–104. doi:10.1016/j.isprsjprs.2011.11.002

Rothlisberger, J.D., Finnoff, D.C., Cooke, R.M., Lodge, D.M., 2012. Ship-borne Nonindigenous Species Diminish Great Lakes Ecosystem Services 462–476. doi:10.1007/s10021-012-9522-6

Saatchi, S., Buermann, W., ter Steege, H., Mori, S., Smith, T.B., 2008. Modeling distribution of Amazonian tree species and diversity using remote sensing measurements. Remote Sens. Environ. 112, 2000–2017. doi:10.1016/j.rse.2008.01.008

Sadro, S., Gastil-Buhl, M., Melack, J., 2007. Characterizing patterns of plant distribution in a southern California salt marsh using remotely sensed topographic and hyperspectral data and local tidal fluctuations. Remote Sens. Environ. 110, 226–239. doi:10.1016/j.rse.2007.02.024

Scarpace, F.L., Quirk, B.K., Kiefer, R.W., Wynn, S.L., 1981. Wetland Mapping From Digitized Aerial-Photography. Photogramm. Eng. Remote Sensing 47, 829–838.

Sierszen, M.E., Morrice, J.A., Trebitz, A.S., Hoffman, J.C., Sierszen, M.E., Morrice, J.A., Trebitz, A.S., Hoffman, J.C., Sierszen, M.E., Morrice, J.A., Trebitz, A.S., Hoffman, J.C., 2017. Aquatic Ecosystem Health & Management A review of selected ecosystem services provided by coastal wetlands of the Laurentian Great Lakes A review of selected ecosystem services provided by coastal wetlands of the Laurentian Great Lakes 4988. doi:10.1080/14634988.2011.624970

Silva, T.S.F., Costa, M.P.F., Melack, J.M., Novo, E.M.L.M., 2008. Remote sensing of aquatic vegetation: theory and applications. Environ. Monit. Assess. 140, 131–145. doi:10.1007/s10661-007-9855-3

Simard, M., Saatchi, S.S., De Grandi, G., 2000. The use of decision tree and multiscale texture for classification of JERS-1 SAR data over tropical forest. IEEE Trans. Geosci. Remote Sens. 38, 2310–2321. doi:10.1109/36.868888

Smith, S. 1987. Typha: its taxonomy and the ecological significance of hybrids. Archiv fu¨r Hydrobiologie 27:129–38.

Streutker, D.R., Glenn, N.F., 2006. LiDAR measurement of sagebrush steppe vegetation heights. Remote Sens. Environ. 102, 135–145. doi:10.1016/j.rse.2006.02.011

Tapsall, B., Milenov, P., Tasdemir, K., 2010. Analysis of Rapideye Imagery for Annual Landcover Mapping As an Aid To European Union (Eu) Common Agricultural Policy. 100 Years ISPRS - Adv. Remote Sens. Sci. XXXVIII, 568–573. doi:10.5194/isprsarchives-XL-7-195-2014

Templer, P., Findlay, S., Wigand, C., 1998. Sediment chemistry associated with native and non-native emergent macrophytes of a Hudson River marsh ecosystem. Wetlands 18, 70–78. doi:10.1007/BF03161444

Tuchman, N.C., Larkin, D.J., Geddes, P., Wildova, R., Jankowski, K., Goldberg, D.E., 2009. Patterns of environmental change associated withTypha xglauca invasion in a Great Lakes coastal wetland. Wetlands 29, 964–975. doi:10.1672/08-71.1

Underwood, E.C., Klinger, R., Moore, P.E., 2004. Predicting patterns of non-native plant invasions in Yosemite National Park, California, USA. Divers. Distrib. 10, 447–459. doi:10.1111/j.1366-9516.2004.00093.x

Vaclavik, T., and R. K. Meentemeyer. 2012. Equilibrium or not? Modelling potential distribution of invasive species in different stages of invasion. Diversity and Distributions 18:73–83.

Valle, M., Borja, ??ngel, Chust, G., Galparsoro, I., Garmendia, J.M., 2011. Modelling suitable estuarine habitats for Zostera noltii, using Ecological Niche Factor Analysis and Bathymetric LiDAR. Estuar. Coast. Shelf Sci. 94, 144–154. doi:10.1016/j.ecss.2011.05.031

Van Beijma, S., Comber, A., Lamb, A., 2014. Random forest classification of salt marsh vegetation habitats using quad-polarimetric airborne SAR, elevation and optical RS data. Remote Sens. Environ. 149, 118–129. doi:10.1016/j.rse.2014.04.010

Vierling, K.T., Vierling, L.A., Gould, W.A., Martinuzzi, S., Clawges, R.M., 2008. Lidar: Shedding new light on habitat characterization and modeling. Front. Ecol. Environ. 6, 90–98. doi:10.1890/070001

Vierling, L.A., Vierling, K.T., Adam, P., Hudak, A.T., 2013. Using satellite and airborne LiDAR to model woodpecker habitat occupancy at the landscape scale. PLoS One 8. doi:10.1371/journal.pone.0080988

Villamagna, A.M., Murphy, B.R., 2010. Ecological and socio-economic impacts of invasive water hyacinth (Eichhornia crassipes): A review. Freshw. Biol. 55, 282–298. doi:10.1111/j.1365-2427.2009.02294.x

Villero, D., Pla, M., Camps, D., Ruiz-Olmo, J., Brotons, L., 2017. Integrating species distribution modelling into decision-making to inform conservation actions. Biodivers. Conserv. 26, 251–271. doi:10.1007/s10531-016-1243-2

Vitousek, Peter M., et al., 1987. Biological invasion by Myrica faya alters ecosystem development in Hawaii.". Science (80-.). 238, 802–804.

Vitousek, P.M., D'Antonio, C.M., Loope, L.L., Rejmánek, M., Westbrooks, R., 1997. Introduced species: A significant component of human-caused global change. N. Z. J. Ecol. 21, 1–16. doi:10.1890/02-0571

West, A.M., Kumar, S., Brown, C.S., Stohlgren, T.J., Bromberg, J., 2016. Field validation of an invasive species Maxent model. Ecol. Inform. 36. doi:10.1016/j.ecoinf.2016.11.001

Wisz, M., Pottier, J., Kissling, W., Pellissier, L., Lenoir, J., Damgaard, C., C. Forschhammer, M., Grytnes, J.A., Guisan, A., Heikkinen, R., Høye, T., Kühn, I., Luoto, M., Maiorano, L., Nilsson, M.-C., Normand, S., Öckinger, E., Schmidt, N., Svenning, J.-C., 2012. The role of biotic interactions in shaping distributions and realized assemblages of species: implications for species distribution models., Biological Reviews.

Yackulic, C.B., Chandler, R., Zipkin, E.F., Royle, J.A., Nichols, J.D., Campbell Grant, E.H., Veran, S., 2013. Presence-only modelling using MAXENT: When can we trust the inferences? Methods Ecol. Evol. 4, 236–243. doi:10.1111/2041-210x.12004

Zedler, J.B., Kercher, S., 2004. Causes and consequences of invasive plants in wetlands: Opportunities, opportunists, and outcomes. CRC. Crit. Rev. Plant Sci. 23, 431–452. doi:10.1080/07352680490514673

Zhu, B., Ellis, M.S., Fancher, K.L., Rudstam, L.G., 2014. Shading as a control method for invasive European frogbit (Hydrocharis morsus-ranae L.). PLoS One 9. doi:10.1371/journal.pone.0098488

Zhu, B., Ottaviani, C.C., Naddafi, R., Dai, Z., Du, D., 2018. Invasive European frogbit (Hydrocharis morsus-ranae L.) in North America: an updated review 2003–16. J. Plant Ecol. 11, 17–25. doi:10.1093/jpe/rtx031

APPENDIX A

Chapter 1 Appendices

Table A.1.1 Error Matrix for Optical-Only Random Forest Model (RF1)

	Reference Class												
Prediction class	DS	EF	FD	FL	FS	HC	MS	OB	OW	WS	WG	Total	User's Accuracy (%)
Dry Shrub	17	0	0	0	2	0	3	0	0	3	0	25	0.68
Emergent/floating	0	22	0	2	1	0	1	0	0	1	0	27	0.81
Field	0	0	17	0	2	0	4	0	0	1	5	29	0.59
Floating leaf	0	1	0	20	0	0	0	0	0	0	0	21	0.95
Forest	3	0	1	0	22	0	0	0	0	0	0	26	0.85
Hybrid cattail	1	0	0	0	1	24	2	0	0	1	0	29	0.83
Mixed sedge	0	1	4	0	1	3	24	0	0	1	1	35	0.69
Open bulrush	0	0	0	0	0	0	0	30	1	0	0	31	0.97
Open water	0	0	0	0	0	0	0	0	29	0	0	29	1
Wet Shrub	0	0	0	0	0	3	1	0	0	15	0	19	0.79
Wet grass meadow	0	0	8	0	1	0	0	0	0	0	28	37	0.76
Total	21	24	30	22	30	30	35	30	30	22	34	248	
Producer's Accuracy (%)	0.81	0.92	0.57	0.91	0.73	0.8	0.69	1	0.97	0.68	0.82		

Table A.1.2 Error Matrix for SAR-Only Random Forest Model (RF2)

	Reference Class												
Prediction class	DS	EF	FD	FL	FS	HC	MS	OB	OW	WS	WG	Total	User's Accuracy (%)
Dry Shrub	17	0	2	0	1	0	0	0	0	1	1	22	0.77
Emergent/floating	0	14	0	1	0	0	0	0	0	0	0	15	0.93
Field	0	0	25	0	0	0	0	0	0	1	3	29	0.86
Floating leaf	0	3	0	15	0	0	0	4	0	0	0	22	0.68
Forest	2	0	0	0	24	1	3	0	0	2	0	32	0.75
Hybrid cattail	2	0	0	0	0	26	3	0	0	1	0	32	0.81
Mixed sedge	0	0	0	3	1	0	26	0	0	5	0	35	0.74
Open bulrush	0	5	0	3	1	0	0	23	0	0	0	32	0.72
Open water	0	2	0	0	0	0	0	1	30	0	0	33	0.91
Wet Shrub	0	0	0	0	0	3	2	0	0	12	0	17	0.71
Wet grass meadow	0	0	3	0	3	0	1	2	0	0	30	39	0.77
Total	21	24	30	22	30	30	35	30	30	22	34	242	
Producer's Accuracy (%)	0.81	0.58	0.83	0.68	0.8	0.87	0.74	0.77	1	0.55	0.88		

Table A.1.3 Error Matrix for Single Date SAR (August VV and VH) Combination Random Forest Model (RF3)

	Reference Class												
Prediction class	DS	EF	FD	FL	FS	HC	MS	OB	OW	WS	WG	Total	User's Accuracy (%)
Dry Shrub	18	0	1	0	1	0	1	0	0	1	0	22	0.82
Emergent/floating	0	21	0	3	0	0	3	0	0	1	0	28	0.75
Field	0	2	28	0	2	0	0	0	0	0	4	36	0.78
Floating leaf	0	1	0	19	0	0	0	0	0	0	0	20	0.95
Forest	2	0	0	0	24	0	0	0	0	0	0	26	0.93
Hybrid cattail	1	0	0	0	1	26	1	0	0	1	0	30	0.87
Mixed sedge	0	0	0	0	1	0	27	1	0	2	1	32	0.84
Open bulrush	0	0	0	0	0	0	0	29	0	0	0	29	1
Open water	0	0	0	0	0	0	0	0	30	0	0	30	1
Wet Shrub	0	0	1	0	0	4	3	0	0	17	0	25	0.68
Wet grass meadow	0	0	0	0	1	0	0	0	0	0	29	30	0.97
Total	21	24	30	22	30	30	35	30	30	22	34	268	
Producer's Accuracy (%)	0.86	0.88	0.93	0.86	0.8	0.87	0.77	0.97	1	0.77	0.85		

Table A.1.4 Error Matrix for Full-Input Random Forest Model (RF4)

	Reference Class												
Prediction class	DS	EF	FD	FL	FS	HC	MS	OB	OW	WS	WG	Total	User's Accuracy (%)
Dry Shrub	17	0	0	0	2	0	1	0	0	2	0	22	0.77
Emergent/floating	0	23	0	2	1	0	0	0	0	0	0	26	0.88
Field	0	0	29	1	0	0	0	0	0	0	2	32	0.91
Floating leaf	0	1	0	19	0	0	0	0	0	0	0	20	0.95
Forest	3	0	0	0	24	0	0	0	0	0	0	27	0.89
Hybrid cattail	1	0	0	0	0	27	0	0	0	2	0	30	0.90
Mixed sedge	0	0	0	0	1	2	32	0	0	3	0	38	0.84
Open bulrush	0	0	0	0	0	0	0	30	0	0	0	30	1
Open water	0	0	0	0	0	0	0	0	30	0	0	30	1
Wet Shrub	0	0	1	0	0	1	2	0	0	15	0	19	0.79
Wet grass meadow	0	0	0	0	2	0	0	0	0	0	32	34	0.94
Total	21	24	30	22	30	30	35	30	30	22	34	278	
Producer's Accuracy (%)	0.81	0.96	0.97	0.86	0.8	0.9	0.91	1	1	0.68	0.94		

Table A.1.5 Error Matrix of the Full-Input Maximum Likelihood Estimation Classification (MLE)

	Reference Class												
Prediction class	DS	EF	FD	FL	FS	HC	MS	OB	OW	WS	WG	Total	User's Accuracy (%)
Dry Shrub	18	0	0	0	8	0	1	0	0	0	0	27	0.67
Emergent/floating	0	21	0	3	0	0	0	0	0	0	0	24	0.88
Field	0	0	26	0	0	0	0	0	1	0	3	30	0.87
Floating leaf	0	3	0	19	1	0	0	0	0	0	0	23	0.83
Forest	2	0	1	0	21	1	3	2	0	0	0	30	0.70
Hybrid cattail	1	0	0	0	0	27	3	0	0	3	0	34	0.79
Mixed sedge	0	0	0	0	0	0	28	0	0	3	0	31	0.90
Open bulrush	0	0	0	0	0	0	0	28	1	0	0	29	0.97
Open water	0	0	0	0	0	0	0	0	28	0	0	28	1
Wet shrub	0	0	0	0	0	2	0	0	0	16	0	18	0.89
Wet grass meadow	0	0	3	0	0	0	0	0	0	0	31	34	0.91
Total	21	24	30	22	30	30	35	30	30	22	34	263	
Producer's Accuracy (%)	0.86	0.88	0.87	0.86	0.7	0.9	0.8	0.93	0.93	0.73	0.91		

Appendix A.2, Chapter 1 R Script

```
###Partition the full ENVI subset into 70% training and 30% testing datasets###
alldata <- read.csv(file.choose())
library(caret)
library(randomForest)
train.index <- createDataPartition(alldata$ROI_NAME, p = .7, list = FALSE)
train <- alldata[ train.index,]
test  <- alldata[-train.index,]
write.table(x = test, file = "C:/testing.txt")
write.table(x = train, file = "C:/training.txt")
### Convert .txt to CSV###
###Load in the training partition###
RFtrain<-
as.data.frame(read.csv("Q:\\Chapter1Data\\TrainingTestingData\\TrainingRF\\trainingRF
.csv"))
head(yourdata)
###Prepare dataset for RF format###
head(RFtrain)
RFclean<-as.data.frame(RFtrain)
head(RFclean)
RFdata <- RFclean[,c(4:15)]
RF<- randomForest(as.factor(name) ~., data=RFdata, importance=TRUE,
na.action=na.omit)
```

```
RF

RF$predicted

RF$importance

###Load package for error matrix###

library(caret)

###Prediction & confusion matrix###

RFmatrix <- predict(RF, RFtest)

confusionMatrix(RFmatrix, RFtest$name)
```

APPENDIX B

Chapter 2 Appendices

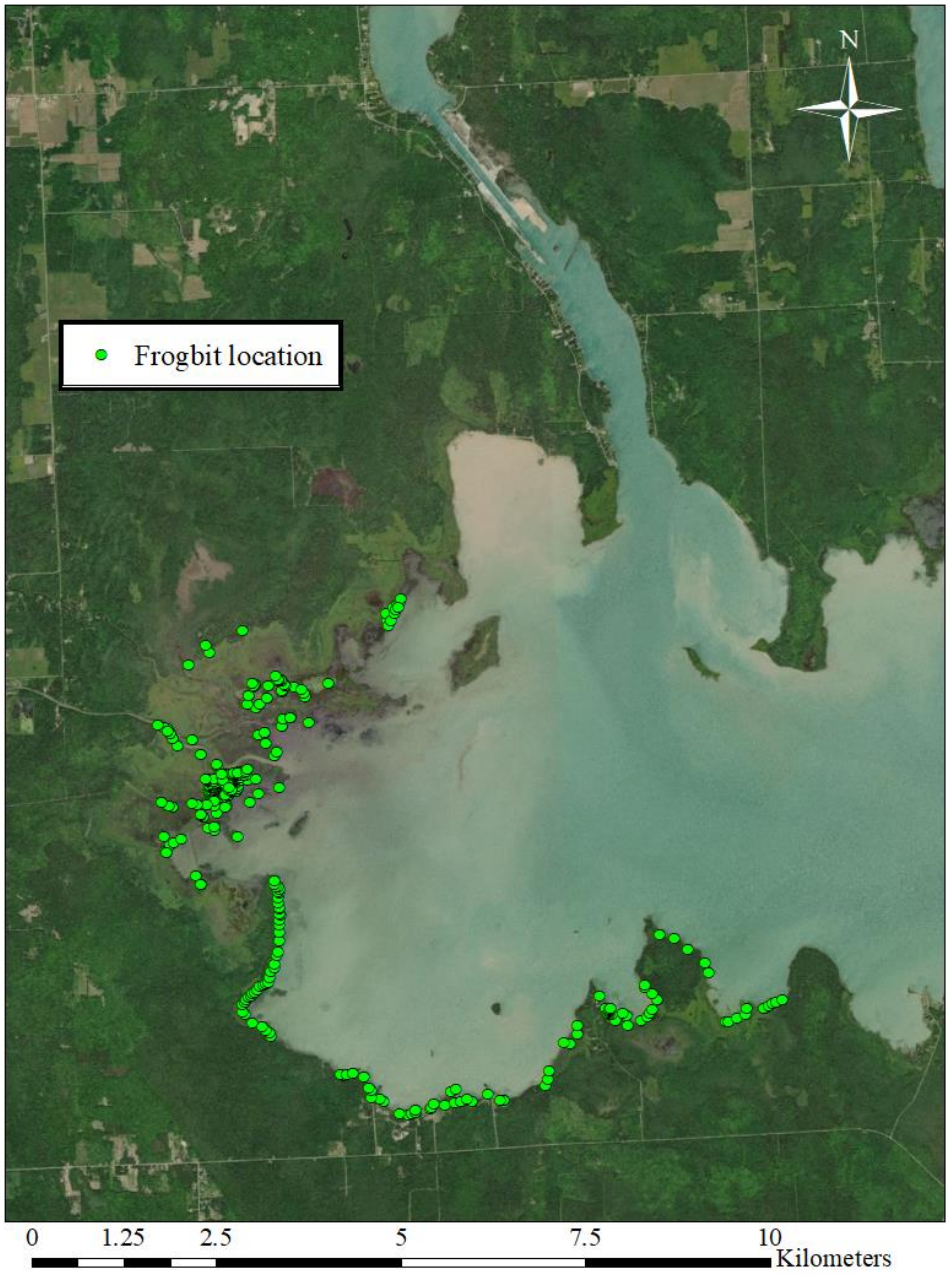

Figure B.1 Locations of Munuscong Bay Frogbit Presences

Table B.1 Pearson's R Correlation between All a *Priori* Covariates. Bolded Numbers Identify a Correlation Coefficient above the 0.70 Threshold

	VegCov	NDRE	JanVV	VegHeight	VVChange	VHChange	EleMin	VegINT	AbsRough	NDVI
VegCov	1	0.65889	0.63541	**0.90871**	0.07122	0.04955	0.68431	**0.85945**	**0.9128**	0.6755
NDRE	0.65889	1	**0.76534**	0.59515	0.10555	0.07309	0.66006	0.60961	0.66069	**0.98971**
JanVV	0.63541	**0.76534**	1	0.573	0.10254	0.06855	0.53639	0.58421	0.62306	**0.77044**
VegHeight	**0.90871**	0.59515	0.573	1	0.05456	0.04194	0.6447	**0.85585**	**0.91665**	0.60699
VVChange	0.07122	0.10555	0.10254	0.05456	1	**0.70601**	0.06572	0.05821	0.06274	0.10721
VHChange	0.04955	0.07309	0.06855	0.04194	**0.70601**	1	0.03504	0.04221	0.04525	0.0747
EleMin	0.68431	0.66006	0.53639	0.6447	0.06572	0.03504	1	0.68939	**0.76664**	0.67406
VegINT	**0.85945**	0.60961	0.58421	**0.85585**	0.05821	0.04221	0.68939	1	**0.96711**	0.62408
AbsRough	**0.9128**	0.66069	0.62306	**0.91665**	0.06274	0.04525	**0.76664**	**0.96711**	1	0.67556
NDVI	0.6755	**0.98971**	**0.77044**	0.60699	0.10721	0.0747	0.67406	0.62408	0.67556	1

Appendix B, Chapter 2 R Script

```
###Load packages###

library(raster) # spatial data manipulation

library(MASS) # for 2D kernel density function

library(magrittr) # for piping functionality, i.e., %>%

library(maptools) # reading shapefiles

###Data preparation###

Frogbitdata <- read.csv(frogbitfinal.csv)

lonlat <- Frogbitdata[, c("X", "Y")]

covdat <- brick(elemincovariate)

occur.ras <- rasterize(lonlat, covdat, 1)

plot(occur.ras)

###Bias layer creation###

presences <- which(values(occur.ras) == 1)

pres.locs <- coordinates(occur.ras)[presences, ]

density <- kde2d(pres.locs[,1], pres.locs[,2], n = c(nrow(occur.ras), ncol(occur.ras)))

        density.ras <- raster(density)

plot(density.ras)

writeRaster(density.ras, "filelocation")
```